# 16 The Qinling–Dabie ultra-high-pressure collisional orogen

B. R. HACKER, X. WANG, E. A. EIDE, and L. RATSCHBACHER

**Abstract**

The Qinling–Dabie orogen of east-central China is showcased by diamond- and coesite-bearing rocks regionally metamorphosed at ultra-high pressures of up to about 4.0 GPa. We review and summarize the diverse literature on the orogen to help geologists new to the area quickly assimilate the existing data. The ultra-high pressure (UHP) rocks occur in a high-grade, penetratively deformed gneiss terrane and do not represent a stratigraphic succession as first described. Strike-slip faults, traditionally considered to be fundamental breaks separating unrelated rocks, are more likely second-order features superimposed on low-angle faults and nappes associated with continental collision. Much of the existing radiometric data must be considered suspect until analytical and petrographic details are available. Care should also be taken in extrapolating fossil ages to rocks far from localities where the fossils were unearthed. Sedimentologic, paleomagnetic, and radiochronologic data all indicate Triassic collision and subsequent Triassic–Jurassic orogenic collapse, but the widespread excess $^{40}Ar$ (particularly in low-K eclogites) and/or other unusual isotopic systematics currently preclude more detailed understanding. Early reports of Precambrian UHP metamorphism are incorrect. Much effort has been focused on the metamorphism of these UHP rocks, but little is known about the structures that may have been active during collision or exhumation.

The current tectonic models are poorly constrained. The possible means for exhumation of the UHP rocks include upward flow during subduction, buoyancy-driven vertical shortening and horizontal extension, vertical extrusion caused by indentation into thermally weakened crust, lateral extrusion, and erosion. Crucial topics awaiting resolution include the following: the timing of partial melting relative to UHP metamorphism; the location and genesis of any subduction-related volcano-plutonic arc; the ages and compositions of the Jurassic and Cretaceous plutons and volcanic rocks, and their relationships to the collisional orogeny; the location and petrogenesis of sediments that must have been derived from the UHP rocks during exhumation; an explanation of the discordance and complexity among the isotopic data on UHP metamorphism; characterization of the rates and magnitudes of displacement along structures responsible for exhumation.

## Introduction

Discovery of regionally extensive terranes of ultra-high-pressure (UHP) metamorphic rock containing coesite and/or diamond (Chopin, 1984; Smith, 1984; Wang, Liou, and Mao, 1989) has inspired new interest in the tectonics of continental collisions. Study of these UHP rocks has raised many exciting questions. How is continental crust subducted to profound depths exceeding 100 km? How and why are UHP metamorphic minerals preserved during decompression and cooling, rather than being converted to more stable minerals? What is the rate of exhumation, and what tectonic processes are responsible for exhumation?

Study of UHP terranes is the most direct means by which to address these questions and glean more information about the physical and chemical properties of the crustal lithosphere during and after collisional orogenesis. Wang and Liou (1991) reported that the Dabie Shan (Mountains) within the Qinling–Dabie orogen of east-central China (Figure 16.1) contain more than 2,500 km$^2$ of continental crust that was subducted during Triassic time to depths of more than 100 km and later exhumed. If so, the Dabie Shan and the related Sulu and Hong'an areas constitute the world's largest example of a UHP orogen and probably should be considered the archetype.

Although the Qinling–Dabie orogen has been extensively investigated by Chinese geologists, most of the published maps and interpretations have not conformed to the geologic conventions that are followed outside of China. Because of the growing recognition that this UHP belt may tell us much about collisional tectonics, geologists outside China may wish to assimilate the existing map and laboratory data and differentiate them from geologic interpretations. One purpose of this chapter is to provide a review of the literature that will make such assimilation possible. Our second intention is to review the preserved geologic structures, rock types, and radiometric ages and analyze their implications for the tectonic history of these UHP rocks. Metamorphism is discussed in only cursory fashion, because of

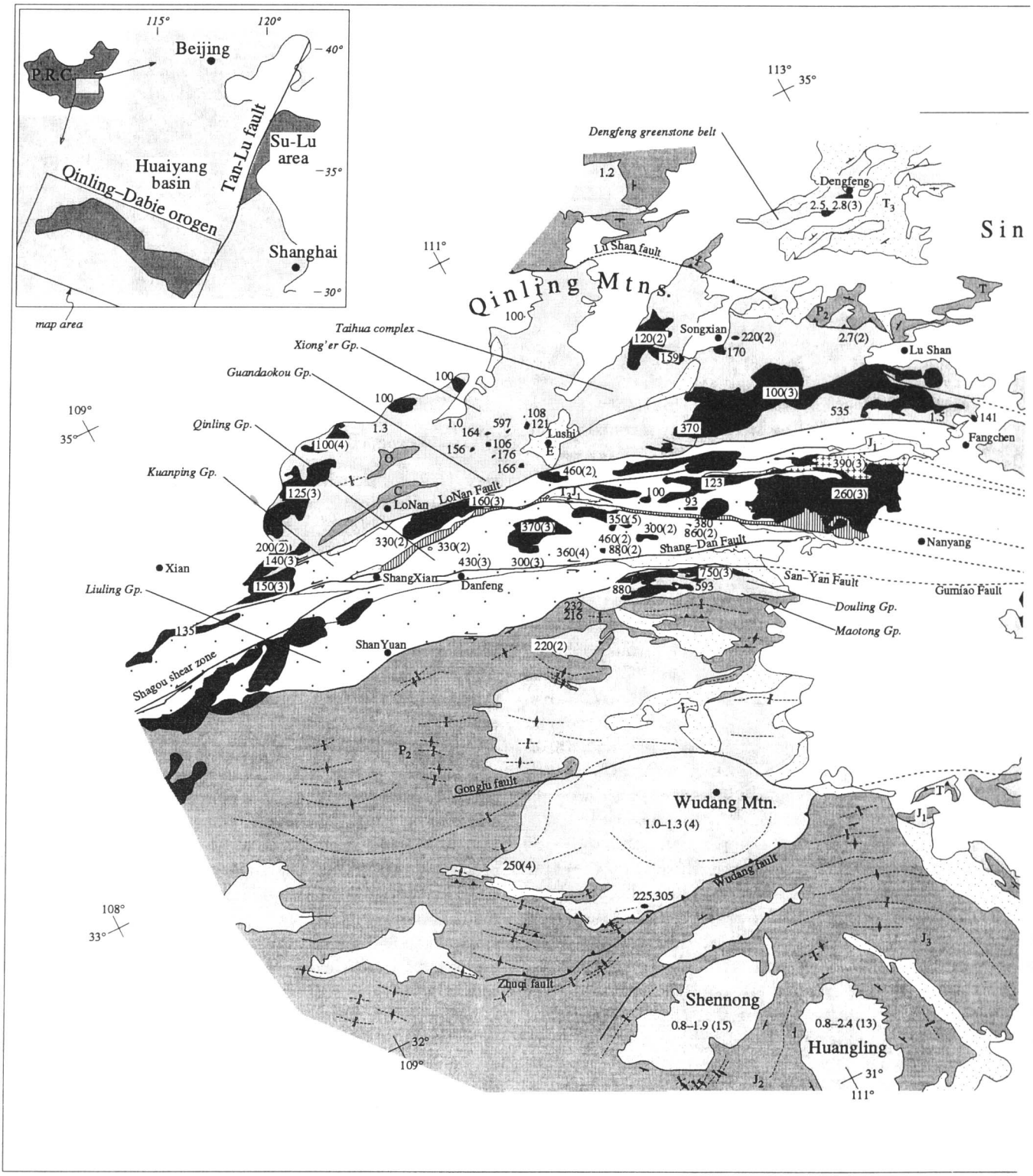


**Figure 16.1 Summary geologic map of the Qinling–Dabie orogen. Numbers signify U-Pb, K-Ar, $^{40}Ar/^{39}Ar$, Sm-Nd, and Rb-Sr ages reported in a wide variety of publications (R.G.S. Anhui, 1987; R.G.S. Henan, 1989; R.G.S. Shaanxi, 1989; Zhang et al., 1989; R.G.S. Hubei, 1990; Li and Wang, 1991; Ames et al., 1993; Li et al., 1993b; You et al., 1993; Hacker and Wang, in press). The ages have been filtered in two ways; (1) Ages from within a given pluton or a given area of about 10 km$^2$ that differ by less than 10% have been averaged (the number of ages that have been averaged is enclosed within parentheses). (2) Some K-Ar and $^{40}Ar/^{39}Ar$ ages from the Dabie Shan have been excluded from this figure for clarity, but are included in Figure 16.2.**

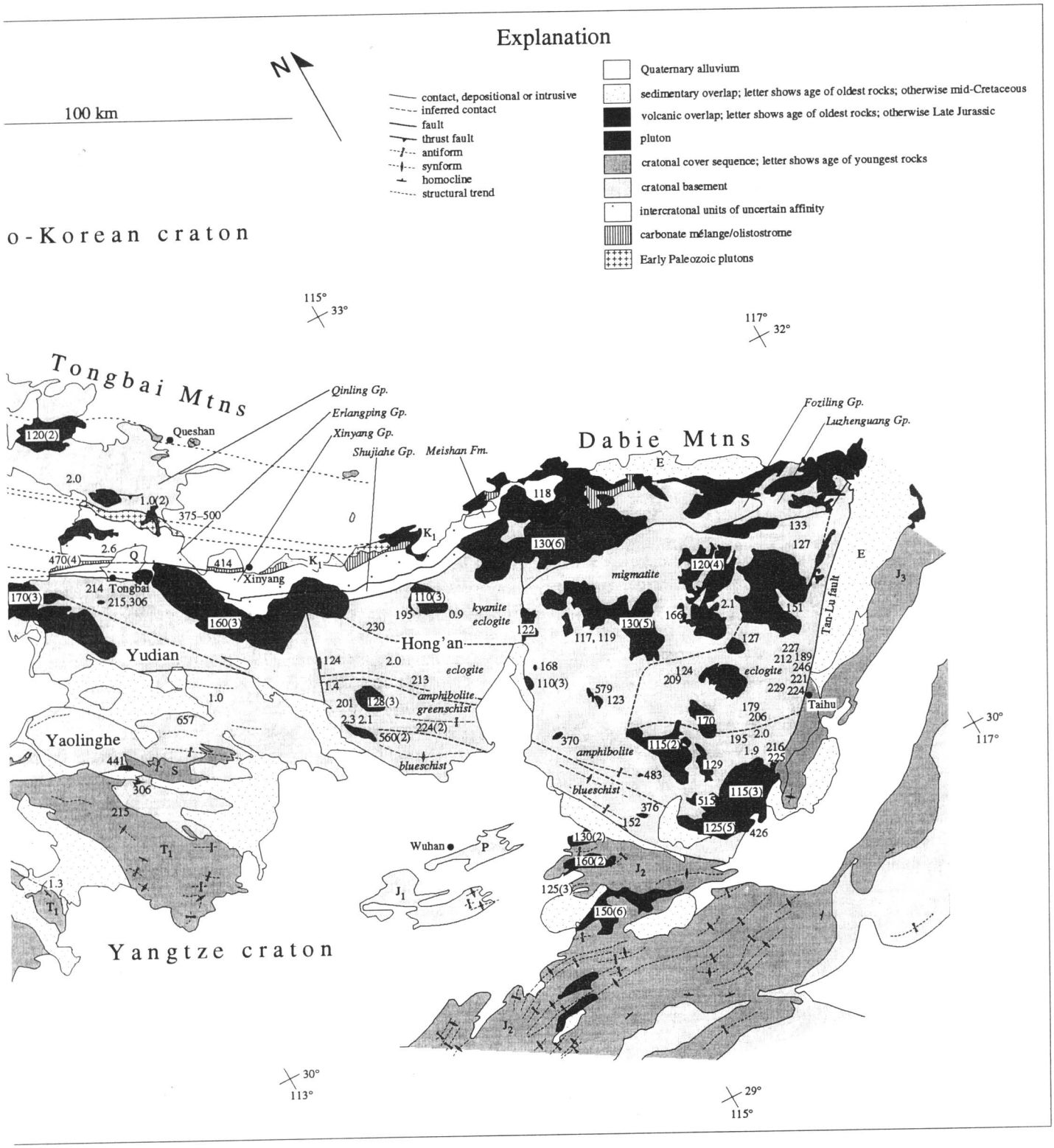


**Figure 16.1.** (*cont.*) **Evaluation of the accuracy or precision of most ages is impossible, because isotope data are not available. Precambrian ages have been rounded to the nearest 0.1 Ga and are shown as two digits separated by a decimal point (e.g., "1.4"); younger ages are given as three digits and in units of Ma. Map data are from our personal observations and from the published literature (R.G.S. Anhui, 1987; R.G.S. Henan, 1989; R.G.S. Shaanxi, 1989; R.G.S. Hubei, 1990; Zhong et al., 1990; Ernst et al., 1991; Ma, 1991; Eide, 1993; Huang, 1993; Kröner et al., 1993; Okay et al., 1993; Zhou et al., 1993). GP., "group."**

the thorough treatment given by Liou et al. (Chapter 15, this volume).

## Regional geology of the Qinling–Dabie orogen

The approximately 2,000-km-long, east–west-trending collision zone between the Sino-Korean and Yangtze cratons is preserved in east-central China. The core of the orogen includes, from west to east, the Qinling, Tongbai, and Dabie Shan (Figure 16.1). The Sulu area, offset about 500 km to the northeast by the Tan Lu fault, contains rocks similar to those in the Dabie Shan (Enami and Zang, 1990; Enami, Zang, and Yin, 1993).

The clearest evidence of continent–continent collision in this orogen derives from the distribution of rocks metamorphosed at high and ultra-high pressures. UHP ( $> 3.8$ GPa) diamond-bearing eclogites in marbles and calc-silicate layers have been reported from two localities in the Dabie Shan (Xu et al., 1992b; Okay, 1993a) (Figure 16.2). UHP coesite-bearing eclogite ( $\sim 3.0$ GPa) crops out in the Dabie Shan, the Sulu region, and the northeastern corner of the Hong'an area (Wang et al, 1989; Eide, 1993; Zhang and Liou, 1994) (Figure 16.1). Coesite-free ecologite is present in the Sulu area and in the main orogen, beginning with a band in the Dabie Shan that narrows westward before disappearing at about 114°E (Eide, 1993) (Figures 16.1 and 16.2). Blueschist- and transitional blueschist/greenschist-facies rocks crop out in a narrow zone in the southernmost Dabie Shan and then widen westward through the southern Hong'an area and into the Yudian and Wudang areas (Ernst et al, 1991; Eide, 1993) (Figures 16.1 and 16.2). Some granulite- and amphibolite-facies rocks in the orogen (areas labeled "migmatite" and "amphibolite" in Figure 16.1) may also have experienced high-pressure (HP) metamorphism.

Peak UHP metamorphic conditions exceeded temperatures of 800°C and pressures of 3.8 GPa, as indicated by the presence of metamorphic diamond (Wang, Liou, and Maruyama, 1992; Enami et al., 1993; Okay, 1993a; Liou et al., Chapter 15, this volume). Metamorphic conditions in the ecologite- through blueschist-facies rocks were commensurately lower. For example, the transitional blueschist/greenschist-facies rocks of the Hong'an area reached conditions of only 400–800 MPa at 300–475°C (Eide, 1993). The spatial distributions and metamorphic conditions of these UHP and HP rocks indicate subduction-zone metamorphism on a regional scale.

## Major rock units of the Qinling–Dabie orogen

Most Chinese maps and descriptions consider the bulk of the Qinling–Dabie orogen to be composed of a stratigraphic sequence of meta-sedimentary rocks, including units now at amphibolite, eclogite, and granulite grades. The use of stratigraphic terms such as "group" and "formation" to describe rock units is widespread. For example, the Dabie "Group" is considered to include as many as nine "formations" with an aggregate thickness of $> 25{,}000$ m [Regional Geological Survey (herafter, R.G.S.) Anhui, 1987; R.G.S. Hubei, 1990]! In the field, however, these rocks are mostly penetratively deformed amphibolite- to granulite-facies paragneisses and orthogneisses of variable shapes and sizes. Mapping of these rocks as stratigraphic units has led to multiple difficulties. The following are a few of the problems we have encountered: (1) Some "formations" show extreme along-strike lithologic variation. (2) Regional structure frequently has been interpreted in terms of a folded sedimentary sequence, even in zones of high metamorphic grade where no relict sedimentary features are present. (3) "Unconformities" have been mapped between supposed meta-sedimentary units inferred to be in depositional contact, because of changes in metamorphic grade or because of correlation with distant, less metamorphosed sedimentary rocks. (4) Unit contacts typically are shown on geologic maps as solid, unbroken lines, whereas in the field these contacts often are not exposed, because of weathering in the subtropical climate.

These fundamental problems with the published geologic maps make it difficult to place confidence in the locations and interpretations of mapped contacts, to determine where, if at all, unconformities are exposed, to determine whether or not a contact is faulted, and to make regional correlations. The group and formation names and their attendant sedimentary implications should be abandoned in the case of the medium- to high-grade metamorphic rocks of the Qinling–Dabie orogen. Rocks metamorphosed at low grades retain sedimentary features; hence stratigraphic nomenclature remains appropriate to describe them. We therefore advocate non-genetic unit names for the rocks described in this chapter, but for those readers familiar with the literature, we often refer to existing group and formation names in the following descriptions.

### *Sino-Korean craton*

The Sino-Korean craton bounds the Qinling–Dabie orogen to the north (Figure 16.1). Portions of the Sino-Korean basement are as old as 3.8 Ga (Liu et al., 1992), although the area in Figure 16.1 contains rocks no older than 2.8–2.5 Ga (Kröner et al., 1988). The craton consists of a basement of Archean to Proterozoic metamorphic rock overlain by a relatively uninterrupted 4–8-km-thick superjacent section of Sinian (late Proterozoic to early Cambrian)

**Figure 16.2. Map and cross section of the Dabie Shan, showing radiometric ages, strike and dip of foliation, structural trend lines, and unit names; note orientation of the "north" arrow. Several possibilities for the contact between the migmatite and eclogite are shown; boundaries between hot-eclogite, cold-eclogite, and amphibolite units in the eastern part of the range are shown with solid lines; the amphibolite-blueschist boundary is dashed. Mattauer et al.'s (1991) sample localities were taken from their 1 : 2,500,000 map and thus are only approximate; (J) and (K) refer to plutons with Jurassic and Cretaceous radiometric ages taken from the Chinese literature (Li and Wang, 1991). Radiometric age determinations are abbreviated as a letter code followed by the age in Ma, followed by the reference in parentheses: H, $^{40}Ar/^{39}Ar$ hornblende; B, $^{40}Ar/^{39}Ar$ biotite; M, $^{40}Ar/^{39}Ar$ muscovite; m, K-Ar muscovite, Sm, Sm-Nd mineral–whole-rock isochron; Rb, Rb-Sr mineral–whole-rock isochron; z, U-Pb zircon. Ar age determinations believed to have been contaminated by excess Ar are italicized. References same as in Table 16.1. Lines above cross section show inferred amounts of exhumation in the various units.**

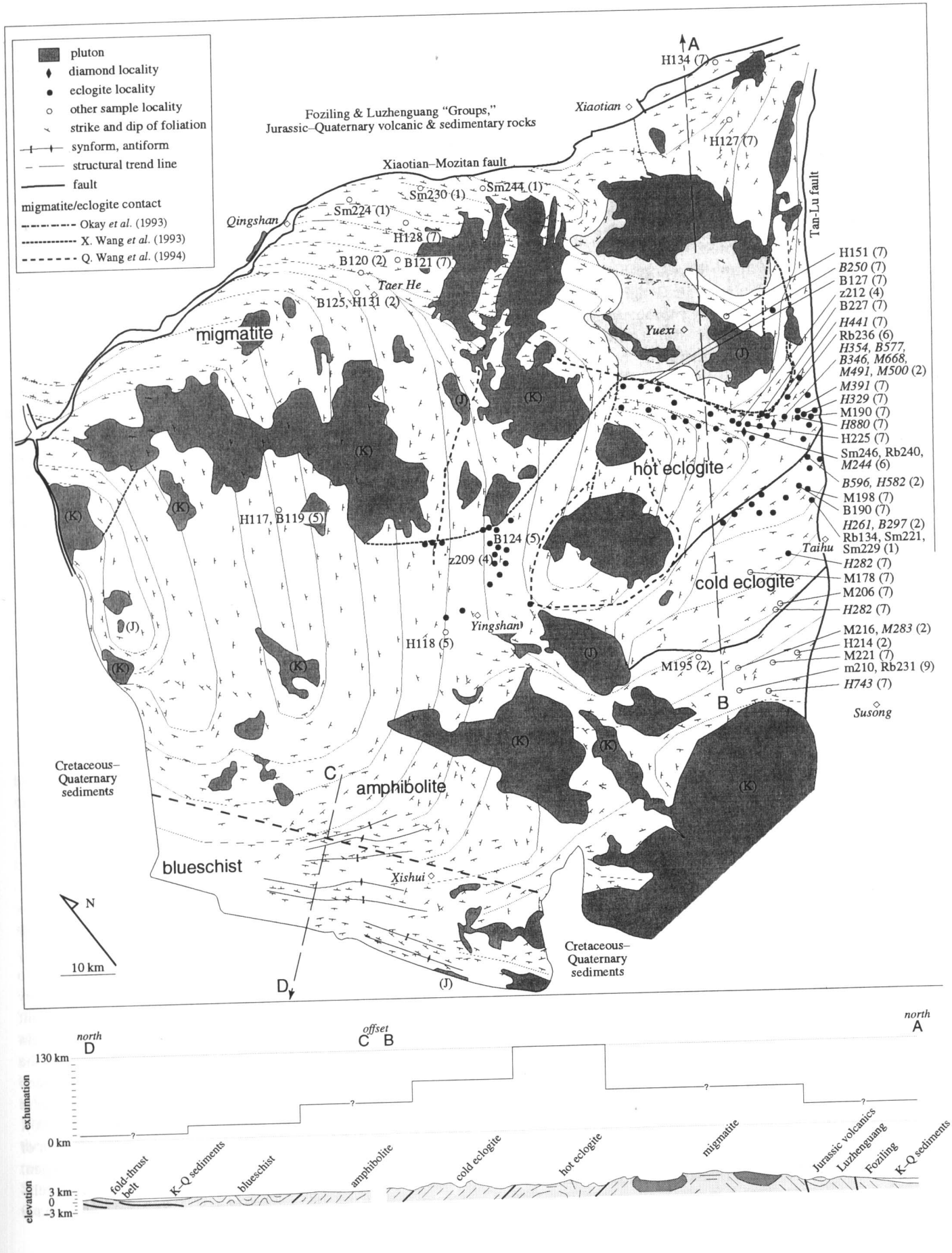
pluton
diamond locality
eclogite locality
other sample locality
strike and dip of foliation
synform, antiform
structural trend line
fault
migmatite/eclogite contact
Okay et al. (1993)
X. Wang et al. (1993)
Q. Wang et al. (1994)
Foziling & Luzhenguang "Groups,"
Jurassic–Quaternary volcanic & sedimentary rocks
Xiaotian–Mozitan fault
Tan-Lu fault
Qingshan
Taer He
Xiaotian
Yuexi
Taihu
Yingshan
Xishui
Susong
migmatite
hot eclogite
cold eclogite
amphibolite
blueschist
Cretaceous–
Quaternary
sediments
H134 (7)
H127 (7)
Sm244 (1)
Sm230 (1)
Sm224 (1)
H128 (7)
B120 (2)
B121 (7)
B125, H131 (2)
H151 (7)
B250 (7)
B127 (7)
z212 (4)
B227 (7)
H441 (7)
Rb236 (6)
H354, B577,
B346, M668,
M491, M500 (2)
M391 (7)
H329 (7)
M190 (7)
H880 (7)
H225 (7)
Sm246, Rb240,
M244 (6)
B596, H582 (2)
M198 (7)
B190 (7)
H261, B297 (2)
Rb134, Sm221,
Sm229 (1)
H282 (7)
M178 (7)
M206 (7)
H282 (7)
M216, M283 (2)
H214 (2)
M221 (7)
m210, Rb231 (9)
H743 (7)
H117, B119 (5)
B124 (5)
z209 (4)
H118 (5)
M195 (2)
A
B
C
D
N
10 km
north
offset
north
130 km
0 km
exhumation
3 km
0
–3 km
elevation
fold-thrust
belt
K–Q sediments
blueschist
amphibolite
cold eclogite
hot eclogite
migmatite
Jurassic volcanics
Luzhenguang
Foziling
K–Q sediments

to Triassic age (Hsü et al., 1987; Ma, 1989; R.G.S. Henan, 1989). Sinian through late Ordovician rocks are platform-facies sandstone, stromatolitic dolomite, limestone, mudstone and rare evaporites, basaltic flows, and pyroclastics. Late Ordovician through early Carboniferous rocks are locally absent. Devonian to Permian (and, locally, Triassic in Henan province) rocks are shallow-marine limestone and dolomite or lacustrine sandstone, mudstone, limestone, gypsum, and coal. All rocks of the craton in the vicinity of the Qinling–Dabie orogen have been at least weakly metamorphosed and deformed into a north-vergent fold-thrust belt (R.G.S. Henan, 1989).

In the area of Figure 16.1, the Sino-Korean craton is composed chiefly of the Taihua complex and the Dengfeng greenstone belt. The Taihua complex comprises amphibolite- to granulite-facies felsic gneiss, migmatite, amphibolite, marble, quartzite, and banded iron formation. The greenstone belt is made up of greenschist- to amphibolite-facies bimodal volcanic rock, ultramafic rock, and terrigenous sedimentary rock. Both units have been intruded by a suite of tonalite-trondhjemite-granodiorite plutons (Zhang et al, 1985; R.G.S. Shaanxi, 1989; Gao et al., 1992; Liu and Shan, 1992). Also interpreted as part of the Sino-Korean craton are various metamorphic rocks of greenschist to amphibolite facies, such as the Xiong'er and Guandaokou "groups." The Xiong'er "Group" comprises 4–9 km of low-greenschist- to amphibolite-facies, calc-alkaline, chiefly andesitic flows, breccia, and tuff. The Guandaokou "Group" includes low-greenschist-facies stromatolitic dolomite, with less sandstone and shale. These "groups" have yielded Proterozoic U-Pb zircon, K-Ar muscovite, and Rb-Sr whole-rock isochron ages (R.G.S. Henan, 1989; R.G.S. Shaanxi, 1989). As discussed later, ages such as these are of uncertain value, because they may be detrital, metamorphic, or crystallization ages.

### *Yangtze craton*

The Yangtze craton forms the southern boundary of the Qinling–Dabie orogen. Like the Sino-Korean craton, it consists of a Precambrian core overlain by dominantly sedimentary, Sinian-to-Mesozoic strata. Basement exposed in the Shennong, Wudang Shan, and Yaolinghe areas (Figure 16.1) includes mafic volcanic/hypabyssal rock, stromatolitic dolomite, terrigenous sandstone, siltstone, and marble, which range from weakly metamorphosed to greenschist facies to blueschist facies, in these three areas, respectively (R.G.S. Hubei, 1990). The Huangling area contains higher-grade migmatitic amphibolite, quartzofeldspathic gneiss, amphibolite, marble, quartzite, and schist (Gao et al., 1992), with zircon ages as old as 2.9 Ga (Hao, 1990; Ames, Zhou, and Xiong, in press). Also interpreted as part of the Yangtze craton are various greenschist- to amphibolite-facies metamorphic units (e.g., the Douling and Maotang "groups" in Figure 16.1) composed of micaceous gneiss and schist, with subordinate hornblende gneiss, quartz keratophyre, pyroclastics, and massive to pillowed Ti-rich basalt (R.G.S. Henan, 1989); these rocks may be Precambrian basement or metamorphosed equivalents of younger cover strata, as discussed next.

Overlying the Precambrian basement are about 12 km of weakly metamorphosed Upper Sinian to Triassic sedimentary rocks. The Upper Sinian is composed of quartzite, phyllite, phosphorite, and dolomite; Cambrian-through-Carboniferous rocks are mostly platform- to shelf-facies mudstone, limestone, feldspathic quartz sandstone, dolomite, and minor volcaniclastic rocks. The only exceptions to these passive-margin sedimentary rocks are Upper Devonian fluvial conglomerate, quartz sandstone, and mudstone in the Yangtze gorge area (southwest of the area in Figure 16.1) that lie unconformably on Silurian rock. Permian platform-facies carbonates give way up-section to coal-bearing clastics and phosphorite deposits indicative of restricted shelf and lagoonal deposition.

### *Syn-collisional to post-collisional overlap assemblage*

Sinian-through-Carboniferous submarine passive-margin sedimentation gave way to Permian deposition of lacustrine and lagoonal sediments in some areas of the Sino-Korean and Yangtze cratons, suggesting a local change in climate or sea level (R.G.S. Anhui, 1987; R.G.S. Henan, 1989; R.G.S. Hubei, 1990). Sediment deposition changed markedly on the Sino-Korean craton in the early Triassic, when lacustrine-to-alluvial conglomerate, arkosic sandstone, and siltstone were laid down; that continental depositional environment persisted on the Sino–Korean cration throughout the Mesozoic. The shift to continental sedimentation occurred on the Yangtze craton in late Triassic time, following early and middle Triassic evaporite, carbonate, and argillite deposition on shallow-marine platforms with restricted circulation. During the Jurassic, continental clastic sedimentation on both cratons continued and was accompanied by deposition of up to 5 km of calc-alkaline, crustal-derived, intermediate-composition of volcanic rocks: tuff, volcanogenic sandstone, and some lava (R.G.S. Anhui, 1987; R.G.S. Henan, 1989; R.G.S. Hubei, 1990). Gneiss cobbles, presumably derived from the Dabie Shan, first appear in the Zhuji Formation on the northern slope of the Dabie Shan from middle Jurassic time (within the "volcanic-overlap" unit of Figure 16.1) (Ma, 1991).

### *Intercratonal units*

Rocks in an east–west-trending belt north of the HP and UHP units (Figure 16.1) have somewhat uncertain affinities. They comprise sedimentary and metamorphic units inferred to represent microcontinents, volcano-plutonic arcs, accretionary wedges, and remobilized cratonal basement and cover, built within the pre-collision Qinling–Dabie ocean or on the margin of the Sino–Korean craton (Zhang et al., 1989). Classically, the strike-slip faults cutting this part of the orogen have been considered to divide the rocks into fundamentally different "groups" of rocks (R.G.S. Henan, 1989; R.G.S. Hubei, 1990). This fault-based division of units has hindered interpretation of the tectonic evolution of the central part of the orogen. Recently, the strike-slip faults have been recognized as relatively young features, and distinctive, offset rock units have

been correlated across them. In conjunction with these new realizations, this part of the orogen has been reinterpreted as a composite of thrust sheets and/or nappes of remobilized basement and cover of the Sino–Korean and Yangtze cratons (Mattauer et al., 1985; Huang and Wu, 1992). The strike-slip faults displaced the earlier nappe/thrust structures, such that the different strike-slip-fault-bounded blocks show different, but repeated, sections of the nappes, some with inverted metamorphic gradients. Because this critical part of the orogen is undergoing a crucial change from traditional to modern interpretation, we generalize these "intercratonal units" as "flysch," "remobilized-craton," and "ophiolite" units.

*Flysch*

"Flysch" is used here to include the Xinyang, Foziling, and Liuling "groups" and the upper part of the Erlangping "Group." The Xinyang "Group" comprises slates, sandstone, conglomerate, amphibolite, and minor carbonate, with blocks containing Cambrian, Ordovician, Silurian, and Devonian fossils in a matrix that has Triassic ammonites (Mattauer et al., 1985; Hsü et al., 1987; You et al., 1993). The Foziling "Group" consists of several kilometers of quartzite and biotite-muscovite quartz schist that reputedly contains Proterozoic microfauna (R.G.S. Anhui, 1987). Where we have observed this unit the metamorphic grade is sufficiently high (upper-greenschist facies) that recognition of microfauna seems unlikely. On the other hand, the Foziling "Group" may include units of different metamorphic grades. The Liuling "Group" contains similar rocks with Devonian fossils (Du, 1986). Because these "flysch" sequences were all metamorphosed under greenschist- to epidote-amphibolite-facies conditions (R.G.S. Henan, 1989), chronologic evidence other than fossil identification is required to determine the depositional and metamorphic ages of these units; such data do not presently exist. Moreover, although these units are often discussed or shown on maps as a single belt, they may be quite different from one another in terms of protolith age or composition, depositional age, and metamorphic or deformational age. Large portions may, in fact, not represent flysch in the classic sense, but may instead be fault-bounded and imbricated wedges of passive-margin sediments derived from either the Sino–Korean or Yangtze craton – in which case these rocks might be better considered as an allochthonous or parautochthonous cratonal cover sequence.

*Remobilized craton*

"Remobilized craton" includes such units as the Kuanping "Group," the Shujiahe "Group," parts of the Qinling "Group," and some "Paleozoic intrusive" rocks. They are chiefly greenschist- to upper-amphibolite-facies quartz-mica schist, biotite gneiss, migmatite, amphibolite, and graphitic marble (Mattauer et al., 1985; R.G.S. Henan, 1989; R.G.S. Shaanxi, 1989; Zhang et al., 1989; You et al., 1993). The protoliths of these rocks may be partly Precambrian, based on Rb-Sr whole-rock and U-Pb zircon ages on gneiss of about 0.9 Ga and an Rb-Sr mineral–whole-rock isochron age on a younger granite of 0.8 Ga (You et al., 1993). As mentioned earlier, the Xiong'er, Guandaokou (R.G.S. Henan, 1989), Douling, and Maotang "groups" (R.G.S. Henan, 1989) also may be remobilized parts of nearby cratons.

*Ophiolite*

"Ophiolite" includes the Danfeng ophiolite, the Zhuzhuang "Group," and the lower part of the Erlangping "Group," which consist of mafic granulite, marble, amphibolite, chert, pyroclastic rock, volcanic flows, dikes, and mélange recrystallized at greenschist-facies conditions (Mattauer et al., 1985; Ma, 1989; R.G.S. Henan, 1989; Wang, 1989; Zhang et al., 1989; Liu and Shan, 1992; You et al., 1993). These ophiolitic rocks contain early Cambrian (?), Ordovician, and Silurian fossils, yield a mix of early Paleozoic isotope ages (Zhang et al., 1989; Li et al., 1990), and are interpreted to be overlain by late Paleozoic sedimentary rocks (Huang and Wu, 1992). Whether this ophiolitic material represents midocean-ridge lithosphere, oceanic-island lithosphere, volcano-plutonic-arc lithosphere, or continental-rift-facies rock has not been determined, but the latter two possibilities are favored over the former (Huang and Wu, 1992).

*Other units*

A carbonate-hosted mélange or olistostrome several kilometers thick crops out from 110°E to 116°E (Figure 16.1). It contains blocks of granite, marble, chert, gneiss, amphibolite, and mylonitic quartzite in a matrix of deformed carbonate-rich rock (Zhong, You, and Suo, 1990; Ma, 1991; You et al., 1993). The extent of this unit and its distinctive lithology make it a key marker unit, and it is shown separately from other "intercratonal units" in Figure 16.1.

The Meishan Formation is a collection of Devonian, low-greenschist-facies carbonates and fossiliferous marine conglomerate, quartz sandstone, and shale in the northern Dabie Shan (Jin, 1989; Ma, 1991) that may be in depositional (Jin, 1989) or fault contact (Ma, 1991) with the underlying Foziling "Group." This unit is important, because if it is depositional on the Foziling "Group" and if the Foziling "Group" turns out to have reached ultra-high pressures, it will provide indisputable documentation of a pre-Devonian age for continental collision.

## Regional structure of the Qinling–Dabie orogen

*Strike-slip faults*

One of the striking features of the Qinling–Dabie orogen, as drawn in Figure 16.1, is the dominance of narrow east–west-trending belts separated by long linear and thus presumably steeply dipping faults. The timing and amount of slip on these features are under debate. Peltzer et al. (1985) proposed left-lateral, Quaternary slip of more than 100 km on the Lo Nan and Shang Dan faults, whereas Huang and Wu (1992) favored the idea of tens of kilometers of displacement on the same faults since the late Cretaceous. The Shang Dan fault may have been a right-lateral strike-slip fault in Cretaceous–Tertiary time, as

indicated by the shapes and distribution of sedimentary basins along it. Mineral stretching lineations and associated fabrics indicate earlier left-lateral displacement and even earlier dip-slip movement (Zhang et al., 1989) associated with formation of an inverted metamorphic gradient in the Liuling "Group" immediately to the south (Hu et al., 1993). The Shagou shear zone deformed granitoid plutons in a sinistral sense at amphibolite-facies temperatures. The time of motion in this zone is bracketed between 126 Ma and 211 Ma by a zircon crystallization age of 211 Ma from a granodiorite protolith and an Sm-Nd garnet–whole-rock age of 126 ± 9 Ma from a rock that contains post-kinematic garnet (Reischmann et al., 1990).

Significantly, none of these probable strike-slip faults offset the Tan Lu fault; see Yin and Nie (1993) for a discussion of this feature. If the latest motion on the Tan Lu fault was Cenozoic (Ma, 1986), this lack of offset is not unexpected. If, however, the last motion on the Tan Lu fault was Cretaceous (Chen et al., 1992), then either (1) the E–W-trending strike-slip faults have not slipped significantly since Cretaceous time or (2) the Huaiyang basin north of the Dabie Shan and west of the Tan Lu fault has been undergoing extension, and the Dabie Shan and Sulu area (inset, Figure 16.1) have been moving eastward (in a relative sense) as a coherent block.

The large strike-slip faults, which appear to be highly significant structures with large displacements, may well be late features with little relevance to the earlier constructional history of the orogen. Moreover, the faults may now juxtapose rocks that are unrelated. Large-scale low-angle faults that were active during construction and collapse of the orogen are likely to be "cryptic" by comparison with these later, more obvious structures. This view is just beginning to bear fruit in the Qinling Shan, where significant thrust faults older than the strike-slip motion have been recognized (Huang, 1993). Large-scale thrust faults have been postulated for the Dabie Shan (Liu and Hao, 1989b; Okay and Şengör, 1992; Xu et al., 1992a), but no well-documented, unambiguous klippen or root zones have been cited as supporting evidence.

### *Folds and other faults*

Few of the faults between units have been investigated to determine age, sense, or magnitude of displacement. Indeed, many of the contacts in the Dabie Shan and Hong'an area that almost certainly must be faults have long been interpreted as depositional (R.G.S. Anhui, 1987). None of the major contacts that we have observed between HP or UHP units in the Dabie Shan and Hong'an area are depositional.

Large portions of the Yangtze and Sino-Korean cratons shown in Figure 16.1 have been thrown into NNW-trending folds and cratonward-directed thrust faults kilometers to millimeters in scale (Mattauer et al., 1985; R.G.S. Henan, 1989; R.G.S. Shaanxi, 1989; R.G.S. Hubei, 1990). For example, the basement and cover of the Yangtze craton were imbricated along south-directed thrust faults in the Wudang Shan area during the mid-Triassic or later (Huang, 1993). Triassic sandstones and slates west of Nanyang show greenschist-facies metamorphism that likely was coeval with formation of the fold-thrust belt (You et al., 1993). Portions of this entire fold-thrust belt also show minor late Jurassic to early Cretaceous movement (R.G.S. Hubei, 1990). In the northern Dabie Shan, for instance, north-directed thrusts have placed older rocks onto Upper Jurassic molasse (Ma, 1989).

Sub-parallel to the major Tan Lu fault (Yin and Nie, 1993) are several NE- to NNE-trending faults. These faults are most evident in maps of the Dabie Shan, but they also separate the Hong'an area from the Dabie and Tongbai Shan. All are steeply inclined and show offsets of Cretaceous and Jurassic plutons on the order of 1 km or less. The two longer faults that bound the Hong'an area may have undergone earlier, larger-magnitude slip, although evidence for this is limited.

## Age of Qinling–Dabie orogenesis

The aforementioned fold-thrust belts reportedly were active between middle Triassic and early Cretaceous time, but what additional constraints are there on the timing of deposition, magmatism, metamorphism, and deformation in the Qinling–Dabie orogen? Most published radiometric ages have proved difficult to evaluate, because many have not included associated analytical data. For example U-Pb zircon ages of 2.9–1.8 Ga have been cited as protolith ages for quartzofeldspathic gneiss in the Dabie Shan, in most cases without a listing of isotope abundances (R.G.S. Anhui, 1987; R.G.S. Henan, 1989; R.G.S. Hubei, 1990). It is impossible to evaluate whether the ages are concordant or might, alternatively, represent mixtures of Triassic metamorphic rims and Precambrian cores, as Ames, Tilton, and Zhou (1993) have shown. In cases where U-Pb ages have been described as upper- or lower-intercept concordia ages, their significance can be partially evaluated. Most published K-Ar, $^{40}Ar/^{39}Ar$, and Rb-Sr ages are also of questionable value because of a lack of published analytical data. Three useful points, however, are apparent from the existing geochronologic data (Figures 16.1 and 16.2):

1. Several dozen Archean to Proterozoic U-Pb and K-Ar ages from the basement of the Yangtze and Sino-Korean cratons are compatible with the Sinian age of overlying cratonal cover sequences. Eight Proterozoic zircon ages from HP and UHP rocks in the Dabie Shan and Hong'an area (R.G.S. Anhui, 1987; R.G.S. Henan, 1989; R.G.S. Hubei, 1990) suggest that these metamorphic rocks may also contain detrital or entrained Proterozoic zircons. This inference is substantiated by upper-intercept U-Pb zircon ages of 856–604 Ma from Dabie eclogite and gneiss and 796–727 Ma from Sulu eclogite and gneiss (Ames, 1993; Ames et al., 1993, in press). Whether these rocks actually crystallized or were deposited in the Proterozoic is unknown.

2. Large numbers of U-Pb and K-Ar ages between about 100 Ma and 130 Ma indicate widespread Cretaceous plutonism throughout the area shown in Figure 16.1, except for the Yangtze craton west of 113°E and south of 33°N. Although the absence of analytical data makes the accuracy of each quoted age suspect,

the large number of Cretaceous ages lends them credence. This inference is substantiated by 18 $^{40}Ar/^{39}Ar$ ages in the 134–118-Ma range obtained on hornblende, mica, and K-feldspar from the Dabie Shan, the Hong'an area (Mattauer et al., 1991; Eide, McWilliams, and Liou, 1994; Hacker and Wang, 1995) and the Sulu area (Chen et al., 1992), and by one biotite Rb-Sr age from the Dabie Shan obtained by Li et al. (1993b) (Figure 16.2). Jurassic U-Pb and K-Ar ages, ranging from 210 Ma to 145 Ma, are less abundant but cover the same areal extent as the Cretaceous ages.

3. Fewer ( ~ 10) of K-Ar and U-Pb ages falling between roughly 500 Ma and 300 Ma have been reported, chiefly from plutons within the southwestern Dabie Shan and from the intercratonal units between 110°E and 115°E (figure 16.1). Again, it is difficult to evaluate the accuracy of these data, but they may reflect magmatism related to an approximately early Paleozoic orogeny. Potential substantiation of this comes from the Tongbai and Qinling Shan, where granulite and foliated tonalite have yielded zircon ages of 435 Ma and 470 Ma (Kröner, Zhang, and Sun, 1993), and granitic plutons have been dated at about 420–400 Ma (Lerch et al., 1994). Muscovite and biotite $^{40}Ar/^{39}Ar$ ages from the Qinling Shan ranging from 348 Ma to 314 Ma have been interpreted to reflect Carboniferous strike-slip motion between the Yangtze and Sino-Korean cratons (Mattauer et al., 1985).

### *Silurian–Devonian orogeny*

There is limited evidence for a Silurian–Devonian mountain-building event in the Qinling–Dabie orogen. Middle Silurian through early Carboniferous rocks are locally absent on the Sino-Korean craton, and Lower and Middle Devonian sediments are missing from certain areas of the Yangtze craton as well. Lerch et al. (1995) and Zhang et al. (1989) reported granitic plutons with late Silurian to early Devonian U-Pb zircon upper-intercept ages from the Qinling Shan, and Mattauer et al. (1985) noted Middle Devonian strata with ultramafic, mafic, and sialic pebbles in the same area. Together, these observations suggest an early Paleozoic orogeny. K-Ar and U-Pb ages in the 500–300-Ma range from the southwestern Dabie Shan and the intercratonal units as far west as Xi'an, as mentioned earlier, conceivably could be related to early Paleozoic tectonism, but the data are too scarce and imprecise to evaluate. Single-zircon-crystal evaporation ages of 435 Ma and 470 Ma reported for granulite and foliated tonalite in the Tongbai Shan (Kröner et al., 1993) are in the correct age range, but may reflect a mix of young crystal rims and old zircon cores. Further evidence for Paleozoic diastrophism is reported by Zhai, Daym and Hacker (1995).

### *UHP Triassic orogeny*

#### *Previous interpretations*

The continent–continent collision that produced HP metamorphism in the Qinling–Dabie orogen was initially assumed to have been Archean or Proterozoic (Dong et al., 1986; Jin, 1989; Dong, 1993), based principally on two interpretations: The first was that the blueschist-facies rocks in the southern Dabie Shan (R.G.S. Anhui, 1987; Sang, Chen, and Shao, 1987; Ma and Zhang, 1988), the Hong'an area (Yang, Cheng, and Wang, 1986), and the Wudang area (R.G.S. Hubei, 1990) are correlative and depositionally overlain by Sinian sedimentary rocks unaffected by HP metamorphism. K-Ar glaucophane "ages" of about 1,200 Ma have been cited in support of this (R.G.S. Henan, 1989). The second was that Proterozoic U-Pb zircon and apatite ages from the Dabie Shan and Hong'an area reflect metamorphism at that time (Xu et al., 1986; R.G.S. Anhui, 1987; R.G.S. Hubei, 1990).

Strict adherence to the first interpretation assumes (1) that there was no more than one HP event, (2) that the correlations from region to region are correct, and (3) that the observed contacts between blueschists and Sinian sediments are depositional. The second interpretation, that Proterozoic zircon and apatite ages are metamorphic, is improbable, largely because a well-documented U-Pb study using multiple zircon fractions from the Dabie Shan interpreted similar data as reflecting a mix of old crystal cores and young rims (e.g., Ames et al., 1993).

Preliminary work by Mattauer et al. (1991) seemed to support a Precambrian age for the continental collision, as they obtained $^{40}Ar/^{39}Ar$ hornblende, biotite, and muscovite ages as old as 685 Ma from a variety of rock types in the eastern Dabie Shan and the Sulu area (Figures 16.2 and 16.3). Those ages were interpreted to be minimum ages for coesite-bearing eclogite formation. Because Mattauer et al. (1991) did not publish release spectra or isochron diagrams for their analyses, rigorous interpretation of their results is impossible. In addition, two Paleozoic Rb-Sr whole-rock ages interpreted as records of HP metamorphism were published by Sang et al. (1987).

#### *Evidence for Triassic collision*

An assessment of the most recent geochronologic data from a number of studies reveals a large number of fully documented late Triassic metamorphic ages (Table 16.1). Li et al. (1989a–c, 1993a,b, 1994) described eight Sm-Nd and two Rb-Sr mineral–whole-rock isochron ages from 209 ± 31 Ma to 243.9 ± 5.6 Ma on ultramafic rock, amphibolite, and eclogite from the Dabie Shan and the Sulu area; the ages were inferred to be metamorphic. Ames et al. (1993, in press) reported seven U-Pb zircon lower-intercept ages from eclogite and gneiss in the Dabie Shan and Sulu area that they inferred to postdate closely the UHP metamorphism. Their most precise ages are 218.5 ± 1.8 Ma and 218.4 ± 2.5 Ma in the Dabie Shan and 221 ± 2.2 Ma in the Sulu area. Maruyama et al (1994) cited an age of 224 ± 8 Ma from an ion-microprobe study of zircons extracted from a rock similar to that analyzed by Ames et al (1993). Phengites from blueschist-facies rocks in the Hong'an area yielded 230–195-Ma $^{40}Ar/^{39}Ar$ ages (Eide et al., 1994). $^{40}Ar/^{39}Ar$ results from the Sulu area revealed three hornblende ages of 213–195 Ma, one muscovite age of 209 Ma, and two biotite and six K-feldspar spectra suggesting cooling below about 500°C at about 220–200

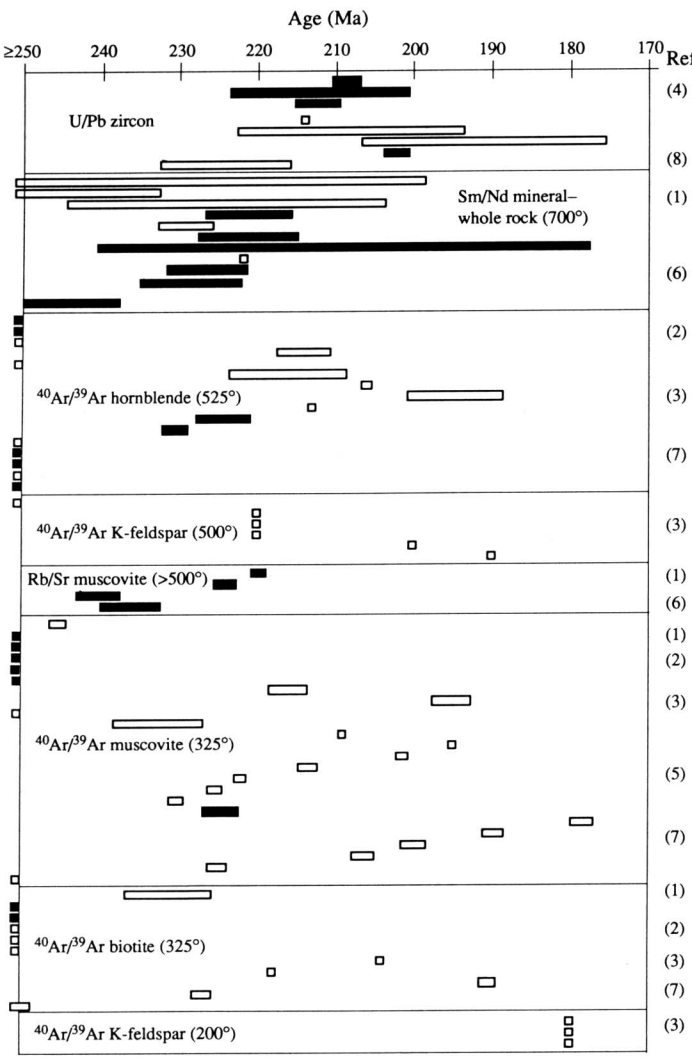


**Figure 16.3. Radiometric ages related to time of UHP metamorphism, shown from highest closure temperature (U-Pb zircon) to lowest closure temperature (K-feldspar, ~ 200°C domain). Bars show reported $2\sigma$ uncertainty of ages; K-feldspar ages come from diffusion-domain interpretations of cyclic-heating experiments, and thus the uncertainties shown are estimates. References same as in Table 16.1**

Ma (Chen et al., 1992). An eclogite from the Dabie Shan yielded externally concordant Sm-Nd, Rb-Sr, and $^{40}Ar/^{39}Ar$ ages of about 244 Ma (Okay, Şengör, and Satir, 1993). Sang et al. (1987) studied amphibolite in the southern Dabie Shan and produced an Rb-Sr mineral–whole-rock isochron age of 231 ± 48 Ma and a K-Ar phengite age of 210 ± 30 Ma. $^{40}Ar/^{39}Ar$ plateau ages of 232 ± 5 Ma and 216 ± 7 Ma on riebeckite and phengite from the fold belt on the northern margin of the Yangtze craton north of Wudang Shan were interpreted by Mattauer et al. (1985) to represent the age of thin-skinned, intracontinental thrusting. Hacker and Wang (1995) also determined eight internally concordant $^{40}Ar/^{39}Ar$ ages on phengite, biotite, and hornblende from amphibolitized eclogite and UHP gneiss from the Dabie Shan ranging from 227 Ma to 179 Ma. Thus, numerous investigators using several isotope systems on different minerals from diverse rock types in disparate areas have produced reliable late Triassic to early Jurassic isotope ages.

Moreover, Hacker and Wang (1995) demonstrated that pre-Triassic $^{40}Ar/^{39}Ar$ ages from Dabie UHP rocks were effects of excess $^{40}Ar$. In addition to their internally concordant data, they found seven other phengite, biotite, and hornblende separates from UHP rocks in the eastern Dabie Shan with strongly discordant release spectra due to excess $^{40}Ar$. Total-gas ages for these discordant samples ranged from about 250 Ma to 880 Ma, and apparent ages of individual steps were as high as 1.5 Ga. Analysis of $^{40}Ar/^{39}Ar$ and $^{40}Ar/^{36}Ar$ ratios for multiple-gas fractions from their samples revealed poorly constrained isochrons, with $^{40}Ar/^{36}Ar$ ratios as high as 30 times the atmospheric ratio of 295.5 and, broadly, late Triassic isochron ages.

Most of the $^{40}Ar/^{39}Ar$ ages older than the Triassic are from eclogite, whereas most of the Triassic–Jurassic $^{40}Ar/^{39}Ar$ ages are from UHP non-eclogitic rocks (Figure 16.3). This may be explained by noting that low-K rocks like eclogite could be significantly influenced by any $^{40}Ar$ in a metamorphic fluid or vapor, whereas K-rich rocks like muscovite-bearing gneiss would necessarily be less affected (Li et al., 1994). This type of widespread contamination renders suspect all existing and future whole-rock and mineral ages from the Dabie Shan derived by the K-Ar method; the $^{40}Ar/^{39}Ar$ method is far more appropriate because of its potential for evaluating the influence of excess Ar.

These data firmly demonstrate that the UHP and HP metamorphism recorded in the Sulu, Dabie, Hong'an, and Qinling areas was late Triassic to early Jurassic in age and that older apparent ages were results of excess $^{40}Ar$ (Hacker and Wang, 1995). However, it would be difficult to justify any further useful interpretations of the isotope ages shown in Figure 16.3. The U-Pb and Sm-Nd ages range from about 240 Ma to about 210 Ma (or, if some outlying data are excluded, perhaps about 235–215 Ma), suggesting that the peak of metamorphism occurred in that time frame. However, more specific regional conclusions cannot reasonably be proposed on the basis of the isotope data in Figures 16.2 and 16.3 and Table 16.1. There is no clear spatial distribution of the ages; the oldest and the youngest Triassic metamorphic ages come from nearby areas in the Dabie Shan. Similarly, although systematic differences among mineral closure temperatures mean that $^{40}Ar/^{39}Ar$ and Rb-Sr ages generally should be younger than U-Pb and Sm-Nd ages, such a trend is not evident in Figure 16.3. In the half-dozen cases in which more than one mineral from a single rock has been analyzed, the expected decrease in ages has been observed in only three cases. The K-feldspar cooling histories modeled by Chen et al. (1992) are not closely matched by the hornblende and mica data, which span a considerable range. Note, moreover, that the suggestion by Yin and Nie (1993) of a westward decrease in $^{40}Ar/^{39}Ar$ ages, from 260 Ma in the Sulu area [chiefly reference 3, but also 1, in Figure 16.3] to 240–208 Ma in the Dabie Shan [references (1), (2), (4), (6), and (7)] is not supported by this larger data set (Hacker and Wang, 1995).

Table 16.1. *Radiometric ages for UHP rocks*

| Sample | Locality | Rock | Mineral[a] | Age (Ma) | Method | Comment[b] |
|---|---|---|---|---|---|---|
| *(1) Li et al. (1989b)* | | | | | | |
| Dzh-1,2 | Dabie Shan | pyroxenite | plag, w.r.? | 230 ± 31 | Sm/Nd | |
| *Li et al. (1993)* | | | | | | |
| R-4 | Dabie Shan | ultramafic | gar, cpx, w.r. | 244 ± 11 | Sm/Nd | |
| G-1 | Dabie Shan | amphibolite | two-gar | 244 ± 20 | Sm/Nd | |
| ND | Dabie Shan | eclogite | gar, cpx | 221 ± 5 | Sm/Nd | |
| T16-1 | Dabie Shan | gneiss | gar, w.r. | 221 ± 5 | Sm/Nd | |
| TiG-1 | Dabie Shan | gneiss | biotite | 231 ± 5 | K/Ar | |
| E87N9-1 | Sulu area | eclogite | gar, cpx | 221 ± 6 | Sm/Nd | |
| E87M1 | Sulu area | eclogite | gar, cpx | 209 ± 31 | Sm/Nd | |
| SJ-1 | Jia Shan | blueschist | phengite | 245.1 ± 0.5 | Ar/Ar | plateau |
| *Li et al. (1994)* | | | | | | |
| QL-1 | Sulu area | eclogite | gar, cpx, w.r. | 226.3 ± 4.5 | Sm/Nd | |
| QL-1 | Sulu area | eclogite | mus, w.r. | 219.5 ± 4 | 0.5 | Rb/Sr |
| QL-1 | Sulu area | eclogite | phengite | 848 | Ar/Ar | excess |
| ZB-4 | Sulu area | eclogite | gar, cpx, w.r. | 228.4 ± 6 | Sm/Nd | |
| ZB-4 | Sulu area | eclogite | mus, w.r. | 223.9 ± 0.9 | Rb/Sr | |
| ZB-4 | Sulu area | eclogite | phengite | 943 | Ar/Ar | excess |
| *(2) Mattauer et al. (1991)* | | | | | | |
| 3 | Dabie Shan | eclogite | amphibole | 345 ± 3 | Ar/Ar | excess |
| 3 | Dabie Shan | eclogite | biotite | 577 ± 6 | Ar/Ar | excess |
| 4 | Dabie Shan | eclogite | phengite | 668 ± 5 | Ar/Ar | excess |
| 5 | Dabie Shan | eclogite | phengite | 491 ± 5 | Ar/Ar | excess |
| 6 | Dabie Shan | eclogite | phengite | 500 ± 5 | Ar/Ar | excess |
| 7 | Dabie Shan | eclogite | amphibole | 582 ± 5 | Ar/Ar | excess |
| 7 | Dabie Shan | eclogite | biotite | 596 ± 5 | Ar/Ar | excess |
| 8 | Dabie Shan | kyanite gneiss | biotite | 297 ± 3 | Ar/Ar | excess |
| 8 | Dabie Shan | kyanite gneiss | amphibole | 261 ± 3 | Ar/Ar | excess |
| 9 | Dabie Shan | quartzite | amphibole | 214 ± 3 | Ar/Ar | plateau? |
| 10 | Dabie Shan | gneiss | amphibole | 283 ± 4 | Ar/Ar | excess |
| 10 | Dabie Shan | gneiss | mus | 216 ± 2 | Ar/Ar | plateau? |
| 10 | Dabie Shan | gneiss | biotite | 300 ± 3 | Ar/Ar | excess |
| 11 | Dabie Shan | quartzite | mus | 195 ± 2 | Ar/Ar | plateau? |
| 12 | Dabie Shan | marble | phlogopite | 346 ± 3 | Ar/Ar | excess |
| ? | Sulu area | ? | mus | 685 | Ar/Ar | excess |
| *Mattauer et al. (1985)* | | | | | | |
| Q134 | Qinling Shan | ? | phengite | 232 ± 5 | Ar/Ar | plateau |
| Q127 | Qinling Shan | ? | riebeckite | 216 ± 7 | Ar/Ar | plateau |
| *(3) Chen et al. (1992)* | | | | | | |
| MH89-7 | Sulu area | ? | K-feldspar | 160, 260 | Ar/Ar | 200°, 500°C domains |
| MH89-11 | Sulu area | ? | K-feldspar | 180, 220 | Ar/Ar | 200°, 500°C domains |
| MH89-12 | Sulu area | ? | K-feldspar | 180, 220 | Ar/Ar | 200°, 500°C domains |
| MH89-13 | Sulu area | ? | K-feldspar | 180, 220 | Ar/Ar | 200°, 500°C domains |
| MH89-13 | Sulu area | ? | biotite | 204 | Ar/Ar | plateau |
| MH89-13 | Sulu area | ? | hornblende | 205.9 ± 0.2 | Ar/Ar | plateau |
| MH89-14 | Sulu area | ? | biotite | 218 | Ar/Ar | plateau |
| MH89-14 | Sulu area | ? | mus | 209 | Ar/A | plateau |
| MH89-16 | Sulu area | ? | K-feldspar | 100, 200 | Ar/Ar | 200°, 500°C domains |
| MH89-31 | Sulu area | ? | hornblende | 194.6 ± 5.5 | Ar/Ar | excess, isochron |
| MH89-37 | Sulu area | ? | hornblende | 213 | Ar/Ar | plateau |
| MH89-32 | Sulu area | ? | K-feldspar | 110, 190 | Ar/Ar | 200°, 500°C domains |
| *(4) Ames et al (in press)* | | | | | | |
| DB-91-28 | Dabie Mtns. | eclogite | zircon | 218.5 ± 1.8 | U/Pb | lower intercept |
| Wumiao | Dabie Mtns. | eclogite | zircon | 214 ± 30 | U/Pb | lower intercept |
| DB-91-34 | Dabie Mtns. | eclogite | zircon | 218.4 ± 2.5 | U/Pb | lower intercept |
| Hu-90 | Tongbai | gneiss | zircon | 226 | U/Pb | lower intercept |
| D-12 | Dabie Mtns. | gneiss | zircon | 218 ± 14 | U/Pb | lower intercept |
| SL-91-7 | Su-Lu area | gneiss | zircon | 177 ± 45 | U/Pb | lower intercept |
| SL-91-28 | Su-Lu area | eclogite | zircon | 221 ± 2.2 | U/Pb | lower intercept |

Table 16.1. (*cont.*)

| Sample | Locality | Rock | Mineral[a] | Age (Ma) | Method | Comment[b] |
|---|---|---|---|---|---|---|
| *(5) Eide et al. (1994)* | | | | | | |
| 91-8A | Hong'an area | gneiss | phengite | 195.2 ± 0.2 | Ar/Ar | plateau |
| 91-22A | Hong'an area | gneiss | phengite | 201.3 ± 0.2 | Ar/Ar | plateau |
| 90-EE-9 | Hong'an area | schist | phengite | 213.3 ± 0.8 | Ar/Ar | plateau |
| 90-EE-26C | Hong'an area | blueschist | phengite | 222.0 ± 0.3 | Ar/Ar | plateau |
| 90-EE-28A | Hong'an area | blueschist | phengite | 225.1 ± 0.4 | Ar/Ar | plateau |
| 90-EE-60 | Hong'an area | gneiss | phengite | 230.1 ± 0.4 | Ar/Ar | plateau |
| *(6)Okay et al. (1993)* | | | | | | |
| 230D | Dabie Shan | eclogite | gar, w.r. | 246 ± 8 | Sm/Nd | |
| 230D | Dabie Shan | eclogite | phengite | 244.3 ± 1.8 | Ar/Ar | exxcess |
| 230D | Dabie Shan | eclogite | phengite, w.r. | 240 ± 2.4 | Rb/Sr | |
| 252C | Dabie Shan | eclogite | phengite, w.r. | 236 ± 3.4 | Rb/Sr | |
| *(7) Hacker and Wang (1995)* | | | | | | |
| 92194 | Dabie Shan | vein in eclogite | hornblende | 230.4 ± 1.1 | Ar/Ar | excess |
| PRC55B | Dabie Shan | amphibolite | hornblende | 282.5 ± 0.9 | Ar/Ar | excess |
| PRC8Oc | Dabie Shan | eclogite | hornblende | 329.5 ± 0.9 | Ar/Ar | excess |
| PRC129d | Dabie Shan | vein in eclogite | hornblende | 440.7 ± 1.2 | Ar/Ar | excess |
| 92PH1 | Dabie San | amphibolite | hornblende | 734.3 ± 1.9 | Ar/Ar | excess |
| PRC81b | Dabie Shan | vein in eclogite | hornblende | 880.1 ± 2.6 | Ar/Ar | excess |
| 92THOL | Dabie Shan | gneiss | phengite | 178.3 ± 0.9 | Ar/Ar | plateau |
| PRC78 | Dabie Shan | gneiss | phengite | 188.6 ± 0.6 | Ar/Ar | plateau |
| PRC131 | Dabie Shan | gneiss | phengite | 199.7 ± 1.0 | Ar/Ar | plateau |
| PRC49d | Dabie Shan | gneiss | phengite | 206.0 ± 0.6 | Ar/Ar | plateau |
| 92SU6A | Dabie Shan | gneiss | phengite | 225.2 ± 0.7 | Ar/Ar | plateau |
| 92H23 | Dabie Shan | gneiss | mus | 391.0 ± 1.1 | Ar/Ar | excess |
| 92127 | Dabie Shan | gneiss | biotite | 190.2 ± 0.6 | Ar/Ar | plateau |
| W92H-1 | Dabie Shan | gneiss | biotite | 228.7 ± 0.7 | Ar/Ar | plateau |
| PRC104b | Dabie Shan | gneiss | biotite | 249.8 ± 0.7 | Ar/Ar | excess |
| *(8) Maruyama et al (1994)* | | | | | | |
| ? | Dabie Shan | gneiss | zircon | 224 ± 8 | U/Pb | (SHRIMP) |
| *(9) Sang et al. (1987)* | | | | | | |
| Rd-19 | Dabie Shan | amphibolite | w.r., mus, plag | 231 ± 48 | Rb/Sr | |
| Rd-19 | Dabie Shan | amphibolite | phengite | 210 ± 30 | K/Ar | |
| Rd-21-28 | Dabie Shan | amphibolites | w.r. | 470 ± 47 | Rb/Sr | |
| Rd-14-20 | Dabie Shan | amphibolites | w.r. | 448 ± 69 | Rb/Sr | |

[a]w.r., whole rock; plag, plagioclase; mus, muscovite; gar, garnet; cpx, clinopyroxene.
[b]plateau, probable plateau age; excess, probably contaminated by excess Ar, based on old apparent age or spectrum shape.

The complexity displayed by the isotope ages from the Dabie Shan may reflect (1) unusual isotope behavior at ultra-high pressures (similar to the age discordance observed in UHP rocks from the Dora Maira massif in the Alps) (Monié and Chopin, 1991; Tilton, Schreyer, and Schertl, 1991) , (2) the presence of excess $^{40}Ar$ in samples with plateau ages, or (3) considerable geologic complexity, such that the samples with different ages are in different fault blocks. Radiometric ages from the well-mapped, eclogite-bearing Western Gneiss Region in Norway are also spatially and temporally complex (Kullerud, Tørudbakken, and Ilebekk, 1986), indicating unexplained isotope and/or geologic complexities at that UHP locality as well.

Inferences drawn from sedimentologic and paleomagnetic data supplement the geochronologic evidence for late Triassic collision. For example, Upper Triassic flysch in the Tongbai Shan marks the first influx of continental material into the pre-collision Qinling ocean (Zhang, Liou, and Coleman, 1984; Hsü et al., 1987). Upper Triassic and younger sedimentary rocks are also less deformed than, and unconformably overlie, older deformed marine strata in the Qinling Shan (Hsü et al., 1987). Recent summaries of paleomagnetic data (Zhao and Coe, 1987; Lin and Fuller, 1990; Enkin et al., 1992) suggest that the Sino-Korean and Yangtze cratons moved farther apart during the middle Permian to middle–late Triassic, but then approached each other between the middle–late Triassic and early Jurassic. Yin and Nie (1993) used the first appearances of clastic

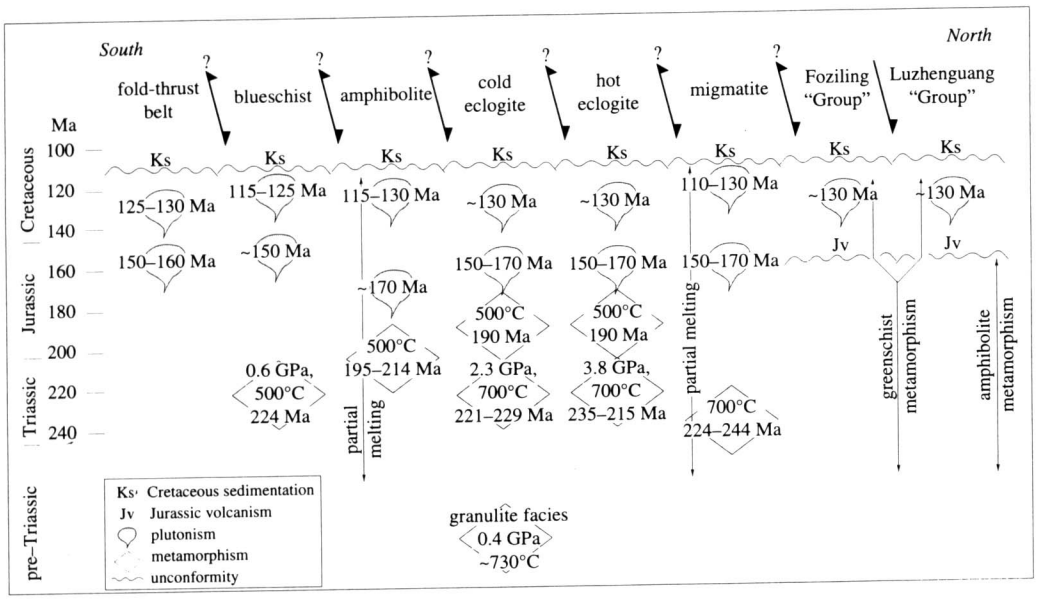


**Figure 16.4. Summary of known geologic relations among units in the Dabie Shan. Ages and senses of motion along faults are poorly constrained. Contact metamorphism, which attains the characteristics of regional metamorphism in some units, is not shown. Arrows for metamorphism and partial melting indicate time intervals over which events could have occurred, not the duration of events.**

sequences overlying thick carbonate sequences along the northern margin of the Yangtze block to infer that collision occurred in middle-to-late Triassic time in the Dabie Shan area.

Triassic continental collisions in China were not limited to the Qinling–Dabie fold belt. Hsü et al. (1990) postulated, on the basis of Lower and Middle Triassic flysch, Middle Triassic depositional hiatuses, and Upper Triassic unconformities, that the Yangtze craton was also involved along it southeast side in a collision with the Huanan block, which underlies much of the Guangxi, Guangdong, and Fujian provinces. The Yangtze craton was the underthrust plate in both collision zones.

### Dabie Shan

The Dabie Shan have been the focus of many investigations of the Qinling–Dabie orogen ever since diamond and coesite were discovered in the core and eastern part of the range (Okay, Xu, and Şengör, 1989; Wang et al., 1989; Xu et al., 1992b). The Dabie Shan are also scientifically attractive because they preserve a potentially informative sequence of rock units that grade northward from a feebly metamorphosed fold-thrust belt through blueschist, amphibolite, and then eclogite overprinted by amphibolite-facies metamorphism, until migmatite is reached in the northern portion of the range (Figures 16.1, 16.2, and 16.4). Here, we describe these main units and their possible contact relationships. We subdivide the Dabie Shan into seven principal units, excluding the carbonate mélange, the low-grade Devonian Meishan Formation, the fold-thrust belt, and the post-Triassic volcanic and sedimentary rocks already discussed. From north to south, these units are the Luzhenguang "Group," the Foziling "Group," migmatite, hot eclogite, cold eclogite, amphibolite, and blueschist. All of these units probably are separated by faults or shear zones, as described later.

All Dabie units are intruded by numerous late plutons of known or probable Cretaceous age. Radiometric ages based on U-Pb zircon and $^{40}Ar/^{39}Ar$ hornblende, biotite, muscovite, and whole-rock analyses span 135 Ma to 110 Ma. Some (but few) intrusive bodies have yielded Jurassic radiometric ages. The plutons are calc-alkalic to alkalic and range from diorite, granodiorite, and granite to minor syenite (R.G.S Anhui, 1987; R.G.S. Henan, 1989; R.G.S. Shaanxi, 1989; R.G.S. Hubei, 1990). Some Mesozoic plutons have truncated earlier structures and are shown on many Chinese maps as "late plutons," whereas others, characterized as "Archean migmatitic plutons," share structures with the country rock. Our observations indicate that a simple twofold partitioning of pluton types is inappropriate, because some granitic bodies have deformed and undeformed portions and are not two separate plutons of different ages. Moreover, "migmatitic" is a misnomer; a more appropriate appellation for such plutons we have examined is "mylonitic," or simply "deformed." Part of this confusion may arise from the fact that the plutons advected considerable heat into the crust during intrusion, with the result that country rocks tens of kilometers distant from exposed plutons reveal Cretaceous $^{40}Ar/^{39}Ar$ ages (Mattauer et al., 1991; Eide et al., 1994; Hacker and Wang, 1995). The gneisses with a Cretaceous thermal overprint, the Cretaceous plutons, and the migmatite unit (described below), however, are distinct, mappable units and must be treated as such.

#### *Foziling unit*

The Foziling "Group" in the Dabie Shan has been correlated with the Xinyang and Liuling "groups" farther west, on the basis of composition, structural position, and the supposed presence of Proterozoic microfauna (R.G.S. Anhui, 1987). The unit is composed of several kilometers of upper-greenschist-facies quartzite and biotite-muscovite quartz schist. The rocks are phyllitic to massive, and the bedding has been transposed into a foliation by millimeter-to-centimeter-scale open folds to isoclinal

folds coincident with cleavage formation. These have been refolded by decimeter-to-decameter-scale folds that postdate cleavage formation (our observations). The foliation strikes subparallel to the axis of the orogen and carries a sub-horizontal mineral stretching lineation (Okay et al., 1993). A Proterozoic protolith age for all of these rocks seems unlikely to us, given the degree of metamorphism and the fact that the Liuling and Xinyang "groups" – also once thought to be Proterozoic–are now recognized as Paleozoic, as discussed earlier. This unit (Foziling) has been interpreted as flysch, but until further sedimentologic work can be completed, that must be regarded as preliminary. The metamorphic age is unknown, but it predates depositionally overlying Jurassic rocks that were only weakly metamorphosed.

### *Luzhenguang unit*

The Luzhenguang "Group" is biotite-bearing granitic gneiss, with minor amphibolite, muscovite-biotite quartz schist, graphitic schist, dolomitic marble, and phosphorite, all recrystallized at amphibolite to greenschist facies (R.G.S. Anhui, 1987; our unpublished observations). Rocks vary from undeformed to greenschist-facies ultramylonites and low-grade cataclasites. The metamorphic and protolith ages are unknown, but predate depositionally overlying Jurassic rocks. The Luzhenguang "Group" shares many characteristics with the migmatite unit immediately to the south, and identification of the differences between these units is needed.

### *Migmatite unit*

The migmatite unit consists of orthogneiss, migmatite, amphibolite, and minor garnet granulite, marble, and ultramafic rock (Wang and Liou, 1991; Okay et al., 1993). No indication of ultra-high pressure have been found; the reported "eclogites" from this unit (e.g., Li et al., 1993b) are actually garnet-diopside skarns or garnet pyroxenites with low-Na pyroxene (our observations; J. G. Liou, personal communication). The orthogneiss is foliated and composed of hornblende (or, less commonly, biotite) plus plagioclase, orthoclase, and quartz, indicating upper-amphibolite-facies metamorphic conditions. Local granulite-facies rocks show garnet, orthopyroxene, and clinopyroxene overprinted by amphibolite-facies minerals (Liou et al., Chapter 15, this volume). The amphibolite contains sphene, but no rutile (Liou et al., Chapter 15, this volume). Zones of partial melting include restites of clinopyroxene, hornblende, biotite, plagioclase, and sphene, with or without garnet, and leucosomes of plagioclase, K-feldspar, quartz, epidote, and muscovite. Deformation textures indicate that the foliation formed at near-solidus temperatures. Mafic dikes cut the partially melted rocks and share some of the foliation developed within their melted host; they may be related to the heat source responsible for the melting. The composition of much of the unit is broadly granodioritic, and the protolith(s) can vary from granodiorite to mafic rock to arkosic metasediment. The age of the protolith(s) is potentially Precambrian, based on U-Pb ages (R.G.S. Anhui, 1987). The only quantitative estimates of metamorphic pressures and temperatures for this unit come from ultramafic rock, for which Wang (1991) postulated retrograde metamorphism beginning at more than 1,000°C and about 2.0 GPa, passing through 900–600°C at pressures of 1.0–1.5 GPa, and then final serpentinization at temperatures below 500°C.

Determination of the age of partial melting in these rocks is weakly constrained. Triassic Sm-Nd mineral–whole-rock isochron ages on ultramafic and amphibolite rock (Li et al., 1993b) indicate that some high-temperature metamorphism occurred at essentially the same time as peak temperatures were reached in the UHP rocks farther south. Thus, partial melting may have predated UHP metamorphism, in which case indications of high pressure may yet be found within the migmatite unit. On the other hand, the partial melting may have followed UHP metamorphism, and the evidence of ultra-high pressures may have been eliminated. Determining this relationship is an important objective of ongoing work. Early Cretaceous $^{40}Ar/^{39}Ar$ hornblende and mica ages (Mattauer et al., 1991; Hacker and Wang, 1995) far from plutons indicate that rocks in the migmatite unit were affected by widespread heating to about 500°C at that time. The pre-Triassic history of this unit is unknown and may have involved additional high-temperature events.

### *Eclogite unit*

The eclogite unit is the only rock unit that preserves evidence of ultra-high pressure, Okay, Şengör, and Satir (1993) subdivided the eclogite-bearing region of the Dabie Shan into "hot eclogite" and "cold eclogite," based on the distributions of coesite and sodic amphibole and inferred metamorphic temperatures. The eclogite unit has been correlated with eclogite-facies rocks in the eastern part of the Hong'an area, where coesite has been found at one locality (Zhang and Liou, 1994). Diamond- and coesite-bearing, eclogite, aragonite-bearing marble, and coesite-free eclogite are found as layers and blocks in quartzofeldspathic orthogneiss and paragneiss, with subordinate amphibolite and metaclastic rock (Wang et al., 1990; Wang and Liou, 1991, 1993; Xu et al., 1992b; Zhang, Liou, and Cong, 1994). The gneiss, which is the most abundant lithology, contains muscovite, quartz, and plagioclase, with variable amounts of epidote, garnet, K-feldspar, biotite, and sphene. It also underwent UHP metamorphism, as indicated by quartz pseudomorphs after coesite in garnet crystals (Wang and Liou, 1991), and spinel partly converted to garnet in ultramafic rock (Wang, 1991; Zhang et al., 1994). The main field distinction between the eclogite-facies gneiss and the migmatite gneiss is the presence of muscovite rather than hornblende in the quartzofeldspathic lithologies.

Petrologic studies have demonstrated that the eclogites and their host rocks underwent a clockwise pressure–temperature evolution, with peak condition of 800 ± 50°C and more than 3.8 GPa for diamond-bearing eclogite, 550–850°C and 2.6–3.2 GPa

for coesite-bearing eclogite, and 635 ± 40°C and 2.3 ± 0.3 GPa for the cold eclogite, which lacks coesite and diamond and contains sodic amphibole (see summary by Liou et al., Chapter 15, this volume). Peak metamorphism was preceded by low-pressure, granulite-facies metamorphism of unknown age (Okay, 1993b). It was followed by greenschist- to amphibolite-facies retrogression at 475–550°C and 500–800 MPa that locally was severe enough to destroy all records of ultra-high pressures (Okay et al., 1989; Wang et al., 1989, 1992; Okay, 1993a; Liou et al., Chapter 15, this volume). Thus, the decompression path involved little or no heating – decompression occurred isothermally or concomitantly with cooling. The chronologic data reviewed earlier indicate that the UHP metamorphism occurred in the range of about 235–215 Ma, and subsequent cooling to temperatures less than 400°C was complete by 190 Ma. Early Cretaceous $^{40}Ar/^{39}Ar$ hornblende and mica ages (Mattauer et al., 1991; Eide et al., 1994; Hacker and Wang, 1995) far from plutons indicate a resurgence of high temperatures related to widespread heat advection by the plutons. The greenschist- to amphibolite-facies retrogression of the eclogite unit may have been related to this Cretaceous plutonism, or it may have been an unrelated event that predated the plutonism. In the latter case, the eclogite unit underwent at least four stages of metamorphism: (1) granulite facies, (2) eclogite facies, (3) amphibolite–greenschist-facies retrogression, and (4) amphibolite–greenschist-facies "contact" metamorphism of regional extent. The protolith age for the eclogite unit is Precambrian, based on U-Pb zircon upper-intercept ages (Ames et al., 1993).

### *Amphibolite unit*

The amphibolite unit (previously part of the Susong "Group") comprises banded muscovite-biotite granitic gneiss, hornblende (± biotite) gneiss, garnet-muscovite schist, garnet amphibolite, marble, kyanite quartzite, metaphosphorite layers, and rare ultramafic lenses (R.G.S. Anhui, 1987; Okay et al., 1993). All are amphibolite- or epidote–amphibolite-facies rocks (Liou et al., Chapter 15, this volume); we have also observed outcrop-scale textures suggesting that the amphibolite was locally partially melted. The protolith age is possibly Precambrian, based on U-Pb ages (R.G.S. Anhui, 1987). The time of regional metamorphism appears to have been late Triassic, based on $^{40}Ar/^{39}Ar$ muscovite ages (Hacker and Wang, 1995), although widespread Cretaceous plutons also led to local contact metamorphism. It is possible that the amphibolite unit grades into the migmatite unit in the western Dabie Shan, although this unit contains rutile, whereas the amphibolite in the migmatite unit has sphene instead (Liou et al., Chapter 15, this volume).

### *Blueschist unit*

The southernmost part of the Dabie Shan (also previously referred to as the Susong "Group"), which may represent the part of the cratonal cover sequence deformed into the fold-thrust belt, contains transitional blueschist/greenschist-facies minerals (Okay et al., 1993). The protolith age must predate Jurassic crosscutting plutons. The time of blueschist-facies metamorphism likely was about 220–200 Ma, based on the metamorphic ages of correlated blueschists in the Hong'an area (Eide et al., 1994). The blueschists in the Hong'an area were metamorphosed at 400–800 MPa and 225–475°C (Eide, 1993); further work will be required to evaluate the protoliths and metamorphic conditions of the Dabie blueschists.

## Internal structure and contacts between Dabie units

Identification and interpretation of the structures responsible for exhumation of the UHP rocks will be essential for clarifying the tectonic history of the Dabie Shan. Unfortunately, because the exhumation occurred from depths in excess of 100 km, it is entirely plausible that structures that were formed early in the exhumation history could later have been annealed, buried by sediments, intruded by plutons, or displaced upward by younger faults and then eroded.

Considerable disagreement exists regarding the internal structure of the Dabie Shan; descriptions of the area range from "several-km-scale recumbent nappes" (Liu and Hao, 1989a) to "regular homoclinal structure" (Okay et al., 1993). A compilation of structural data (1 : 200,000-scale Chinese maps and our own observations) shown in Figure 16.2 illustrates that although no evidence has been presented for recumbent nappes, the structure is not that of a homocline. The NW half of the Dabie Shan, containing chiefly gneiss, migmatite, and minor granulite, includes two multi-kilometer fold-like structures with east-dipping foliations. The SW quarter of the range, mostly blueschist or amphibolite, exhibits a generally SW-dipping foliation folded along regional NNW-trending axes. The southern portion of the mountains is dominated by Cretaceous plutons that significantly disrupt the regional foliation trends in the amphibolite unit. Migmatitic rocks with NE-dipping foliation lie immediately south of the Xiaotian–Mozitan fault in the north-central portion of the range. This foliation is truncated by the Xiaotian–Mozitan fault in the vicinity of Qingshan (Figure 16.2) and either truncates or bends into NE-striking foliation in migmatite in the center of the range. Foliation in the cold-eclogite unit is concordant with that in the more southerly amphibolite unit. The hot eclogite appears to be a large-scale antiform, with foliation changing from an east–west strike in the southern part of the unit to a northwest strike in the northern part; farther west, foliation in the hot eclogite is truncated against the NE-striking foliation in the migmatite unit. These different structural domains and the locally abrupt transitions between them suggest the presence of undiscovered faults or shear zones. Recognizing and documenting these features will be an important focus of our ongoing efforts.

It is difficult to determine the ages of the major known faults in the Dabie Shan because of lack of systematic geochronology for features that truncate or are cut by faults. Existing geologic maps are of questionable value for determining ages of fault motion, because of the significant inconsistencies outlined

earlier. The interpretation of these features has also been hindered by poor exposure. Exceptions to this are the many NNE-trending faults present throughout the Dabie Shan (not shown in the figures because of small displacement). These structures have offsets of 1 km or less, are sub-parallel to the Tan Lu fault, and have produced brittle displacement of Cretaceous plutons; they indicate activity subsequent to about 110 Ma and may be related to the latest motion along the Tan Lu fault.

The following sections document the nature and style of the known contacts in the Dabie Shan. The descriptions are drawn from the cited sources and our own observations and represent as accurately as possible the structural information currently available for this area.

### *Foziling/Luzhenguang contact*

The Foziling "Group" is shown to depositionally overlie the Luzhenguang "Group" on the Anhui-province geologic map (R.G.S. Anhui, 1987) (Figure 16.1). Okay et al. (1993) reported that the contact is a steep fault, although its sinuous map pattern indicates that it may be gently inclined.

### *Xiaotian–Mozitan fault*

The Xiaotian–Mozitan fault (XMF) marks a southward change from subdued, heavily eroded lowlands of the Luzhenguang and Foziling "groups" into the rugged peaks of the migmatite unit (Figure 16.2). We have so far been unable to locate outcrops of the migmatite unit in contact with the Luzhenguang or Foziling units along the XMF because of the weathering induced by the subtropical climate. The topographic expression of the XMF suggests a relatively steep north dip and a WNW strike. Footwall rocks of the migmatite terrane near the fault surface are locally ultramylonitic, with a strong quartz *c*-axis fabric formed at low-amphibolite- to greenschist-facies conditions; that was followed by later brittle cataclastic deformation at lower grade. They contain mineral stretching lineations of ductilely deformed quartz and brittlely deformed K-feldspar that plunge shallowly (5–15°) to the NNW within foliation planes that have variable dip. Composite foliation fabrics defined by quartz, K-feldspar, and biotite suggest that the hanging-wall Luzhenguang moved down toward the northwest. These gently inclined NNW-trending fabrics are discordant with the present steep expression of the WNW-striking XMF and must predate development of the existing fault. The sense of motion during brittle deformation is right-lateral strike slip, as indicated by slickenlines plunging less than 10° to the ESE. This fault is commonly assumed to have experienced early thrust motion (Dong et al., 1993), but our observations do not support that.

Determination of the timing of motion along the XMF is poorly constrained. Jurassic and Cretaceous volcanogenic and molassic rocks are abundant north of the XMF and sparse to the south, compatible with, but not mandating, dip-slip motion in Jurassic–Cretaceous time. Cretaceous plutons are disrupted by brittle fault zones (our observations) along the XMF, implying Cretaceous or later motion at low temperatures. It is most probable that the XMF, as currently defined, is a composite feature including fault strands and shear zones that were active at different times.

### *Migmatite/eclogite fault*

The rugged topography of the migmatite unit changes southward into more gentle mountains of the eclogite unit (Figure 16.2). The fault separating the two units is newly recognized and incompletely explored. At the localities we have investigated (20 km south of Yuexi), a 1-km-thick high-temperature shear zone dips 45–60° southward. The shear zone is localized near plutons of probable Jurassic–Cretaceous age and is dominated by mylonitic orthogneiss derived from the plutons, which themselves contain less deformed cores. It is probable that the motion is syn-plutonic, but constraints on the sense of motion are as yet unavailable. Okay et al. (1993) have made similar observations 10 km west of Yuexi of a "south-dipping band of strongly foliated leucocratic orthogneiss with slices of virtually undeformed coarse-grained granite" and "no clear shear sense." The presence of Cretaceous plutons with similar depths of exposure on either side of this structure implies that the magnitude of post-pluton displacement cannot be large. The extent of this fault across the Dabie Shan is speculative; three possibilities are shown in Figure 16.2. Okay et al. (1993) mapped a NE-striking contact west of Yuexi; Q. Wang et al. (unpublished data) drew a boundary that makes a loop south of Yuexi, extends north toward Taer He, and then turns west toward Yingshan; and X. Wang and Liou (1993) and Dong et al. (1993) inferred a more southerly contact between Yuexi and Yingshan that bends sharply north to follow a large Cretaceous pluton to the northwest corner of the Dabie Shan. Okay et al. (1993) suggested that initially the structure was a north-dipping thrust that later was folded into its present southward dip. All other authors have assumed that the fault between the migmatite and eclogite units is a north-dipping thrust, in which case the fault observed by us and by Okay et al. (1993) may be a different feature.

It is uncertain whether another, probably older, shear zone of more profound displacement might separate the migmatite terrane from the UHP metamorphic rocks. The migmatite unit contains no record of ultra-high pressure; so either the unit never reached high pressures or the high temperatures accompanying migmatization postdated UHP metamorphism and erased mineralogic evidence of great pressure. These two possibilities would require two very different types of fault contacts: (1) If the migmatite terrane never reached high pressures, it must be separated from the UHP rocks by a fault. If the Jurassic–Cretaceous shear zone described earlier represents this structure, the present steep dip of the fault zone may be related to rotation subsequent to juxtaposition of the two major units or may be linked to bending of the footwall during faulting (Buck, 1988; Wdowinski and Axen, 1992). Moreover, the current, southward dip of the fault zone requires that it be a thrust fault. Thrusting is an inefficient means of exhuming UHP rocks,

because the rate of exhumation is limited by the erosion rate, and the low temperatures in the hanging-wall eclogite necessary to preserve coesite could have been achieved only by concomitant deeper-level subduction beneath the eclogite (Hacker and Peacock, 1994). (2) If the migmatite unit was metamorphosed at ultra-high pressure coevally with the eclogite unit, no structure of significant displacement between the two units is required. If that is true, the primary exhumation structure must lie north of the migmatite unit in the area of the XMF.

### *Hot-eclogite/cold-eclogite contact*

The cold-eclogite and hot-eclogite units were distinguished on the basis of differences in metamorphic parageneses and inferred pressures and temperatures (Okay et al., 1993) (Figure 16.2), as discussed earlier. The pressure gap between the two units is inferred to be roughly 1.5 GPa, equivalent to about 45 km of structural thickness. Coesite- and diamond-bearing rocks within the hot-eclogite unit crop out within 15 km of sodic-amphibole-bearing rocks within the cold-eclogite unit (Okay, 1993a). This implies that a fault separates the two units. No structure, however, has been observed. Based on the current observations, three principal possibilities regarding the contact between the units can be proposed. First, if a fault is present and does not predate foliation development, it will necessarily be a south-dipping normal fault (Okay et al., 1993), because the two eclogite units share a common, south-dipping foliation, and the lower-pressure unit is to the south. Second, if the contact predates foliation formation, it can have had any orientation or sense of motion. Finally, the distribution of coesite and diamond used to differentiate between these hot and cold units may be the result of kinetic rather than tectonic processes; a corollary to this is that the transition from hot to cold eclogite might now appear abrupt, either because of a barrier to nucleation of coesite or because of later retrogression, and would not be the result of juxtaposition along a fault.

### *Cold-eclogite/amphibolite-unit contact*

Okay et al. (1993) reported a south-dipping, dip-slip shear zone between the cold-eclogite unit and the overlying amphibolite unit (Figure 16.2). The fine-grained granoblastic gneisses of the eclogite zone pass upward into coarser, unlineated garnet amphibolites and then into a 700-m-thick orthogneiss (Okay et al, 1993). In the same area, we have observed a brittle, cataclastic fault zone developed within mafic rock that separates these two units. If the amphibolite unit did not reach pressures comparable to those in the eclogite – and presently there is no evidence of such – then this structure must also have played a role in exhumation of the UHP rocks.

### *Blueschist-unit contacts*

A south-dipping fault places blueschist-greenschist rocks over amphibolite and gneiss in the southern Dabie Shan (Eide, 1993) (Figure 16.2). Several NNW-trending mylonitic shear zones within the southernmost outcrops of the Dabie Shan warrant further scrutiny, but at present no further data are available. The contact between the blueschist and the fold-thrust belt is likewise little known, in part because of poor exposure (Figure 16.1). Okay et al. (1993) suggested that it is now a post-Cretaceous, south-dipping normal fault.

## Discussion of tectonic models

Two simple facts constrain our understanding of the evolution of the Qinling–Dabie orogen. Following initiation of a subduction zone, rocks in the footwall near the thrust become hotter because of conduction from the hotter hanging wall, while rocks in the hanging wall near the thrust become cooler, for the same reason. Once a steady state has been reached, perturbations in the heat budget of the subduction system, such as subduction of plates of different ages or changes in the convergence rate, can cause heating or cooling of rocks above or below the subduction thrust (Hacker and Peacock, 1994).

Six recognizable types of HP and UHP metamorphic conditions are recorded in the Qinling–Dabie belt (Figure 16.5): Dabie diamond-bearing eclogite formed at about 800°C and more than 3.8 GPa; Dabie coesite eclogite ( ~ 550–850°C and 2.6–3.2 GPa); Dabie cold eclogite ( ~ 635°C and 2.0–2.6 GPa); Hong'an kyanite eclogite ( ~ 600°C and ≥ 1.6 GPa); Hong'an kyanite-free eclogite ( ~ 500°C and 1.0 GPa); and Hong'an blueschist ( ~ 400°C and 0.6 GPa) (Eide, 1993; Okay, 1993a; Liou et al., Chapter 15, this volume). Some protoliths of each of these rocks are demonstrably continental crust; thus, prior to UHP metamorphism they are unlikely to have been deeper than the common thickness of continental crust: 35–50 km (Wever and Sadowiak, 1989). Old continental cratons are cool enough (Morgan, 1984) that the Hong'an blueschist and eclogite could have formed within deep continental crust as a result of heating and fluid influx (e.g., Pearson, O'Reilly, and Griffin, 1991; Jamtveit, Bucher-Nurminen, and Austrheim, 1990) (Figure 16.6A), and need not have formed in a subduction zone (the blueschist and eclogite metamorphic conditions lie at higher temperatures than the "cold continental geotherm" in Figure 16.5). The cold eclogite, coesite eclogite, and diamond eclogite, however, because they were metamorphosed at pressures in excess of 2.0 GPa, must have formed in a collisional orogen where continental crust was cooled and subducted to depths of 70–140 km. If the Hong'an and Dabie rocks both formed in subduction zones, the warmer pressure–temperature ($P$–$T$) array ( ~ 450K/GPa) preserved in the Hong'an rocks relative to that in the Dabie rocks ( ~ 225K/GPa) implies one of three possibilities: (1) the Hong'an and Dabie rocks formed in the same subduction zone, and the Dabie rocks formed later, after the hanging wall had cooled substantially (Figure 16.6B). (2) They formed in different, perhaps adjacent, subduction zones with different thermal structures (Figure 16.6C). (3) They formed in the same subduction zone, and the Hong'an rocks formed later after the hanging wall had been heated sub-

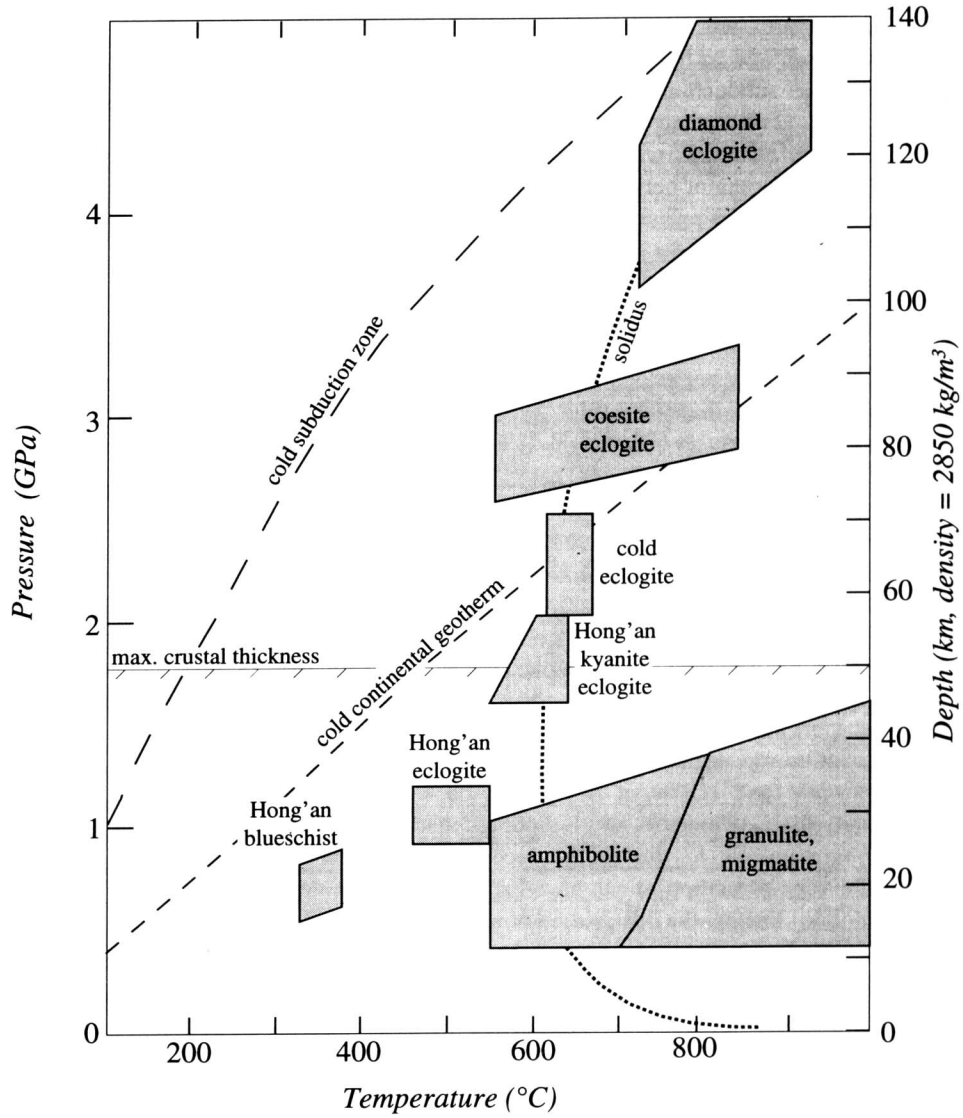


**Figure 16.5. Pressure–temperature conditions of Qinling–Dabie rocks, thermal gradients, and crustal thickness. No time sequence is implied; indeed, amphibolite-facies metamorphism may have occurred more than once. (Adapted from Liou et al., Chapter 15, this volume.)**

stantially – as a result, for example, of ridge subduction (Hacker, 1991). HP and UHP rocks throughout the orogen decompressed isothermally or during cooling (Liou et al., Chapter 15, this volume). While this does not constrain the time interval during which the rocks could have remained at their greatest depths, neither cooling nor heating, it does mandate that all the rocks, from the relatively shallow blueschist to the profoundly deep diamond-bearing eclogite, were insulated from heating during exhumation. That insulation may have been the result of either rapid exhumation or continued subduction at deeper levels while exhumation was occurring.

If the amphibolite and migmatite units of the Dabie Shan underwent early HP or UHP metamorphism and later reached higher temperatures that produced their present parageneses, then they likely formed at depths below the UHP rocks, where rising temperatures could affect them, but not the structurally higher eclogites. Alternatively, if the amphibolite and migmatite units formed at depths less than 40 km, they could not have formed within the same thermal regime as the eclogites, because they represent much higher $P$–$T$ conditions than the eclogites. The amphibolite and migmatite units might have formed in the hanging-wall Sino-Korean craton, where the presence of a continental-margin arc could have produced elevated temperatures at depths of 40 km or less.

### *Existing models*

The existing tectonic models of the Dabie Shan that consider Triassic collision (e.g., Okay and Şengör, 1992; Liou et al., Chapter 15, this volume) are in accord on several basic issues. There is no disagreement that the Yangtze and Sino-Korean cratons are the principal continental colliders, but some models speculatively include intervening microcontinents or intra-oceanic arcs, and the pre-collisional ocean has been shown at various widths (Figure 16.7A). All models assume a north-dipping subduction zone, because the fold-thrust belt in the

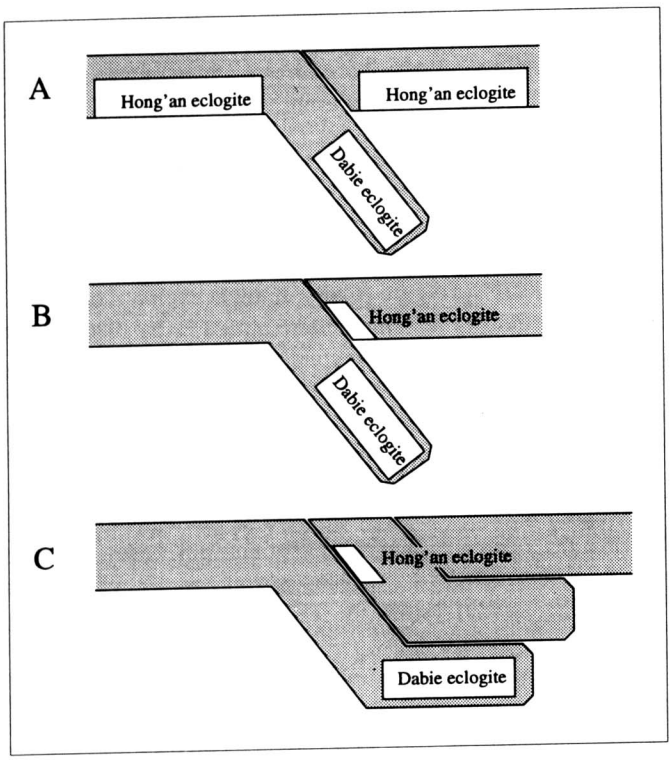


**Figure 16.6. Possible genetic relationships between the Hong'an HP rocks and the Dabie UHP rocks. Crustal thickness shown as 50 km; if the crust is thinner, commensurately more crustal stacking is required.**

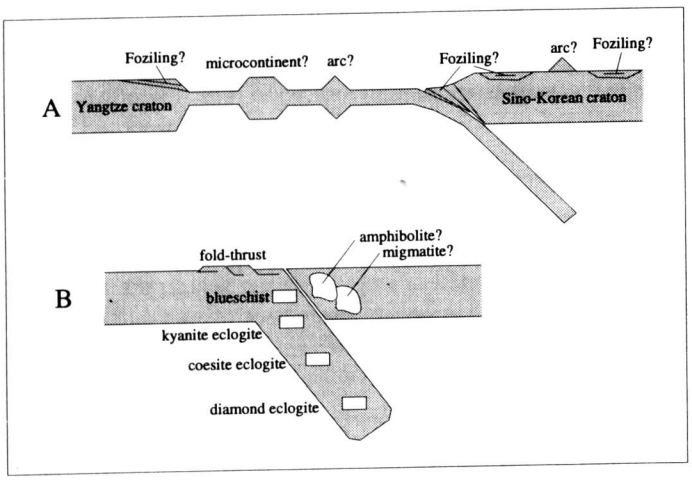


**Figure 16.7. Pre-collisional (A) and collisional (B) tectonic configurations suggested for the Dabie Shan. Crustal thickness shown as 50 km; if the crust is thinner, commensurately more crustal stacking is required. The mantle lithosphere of the upper and middle slabs is assumed to have become detached from the crust.**

southern part of the orogen verges southward, and metamorphic pressures increase northward from blueschist through diamond-bearing eclogite. Volcano-plutonic arcs related to this subduction have been added to the southern margin of the Sino-Korean craton in some tectonic scenarios, but there is only limited evidence for such a feature. Many models assume that the fold-thrust belt, the blueschist unit, and the eclogite unit(s) represent successively more deeply subducted portions of the Yangtze craton (Figure 16.7B,C). These units usually are envisioned to have been exhumed by poorly defined combinations of thrusting at deeper levels and extension at shallower levels, such as proposed by Platt (1986).

All tectonic assumptions must be tested. Diverse tectonic models show the Foziling "Group" as meta-sedimentary rocks deposited before collision in basins on the Sino-Korean craton, on the passive margin of the Yangtze plate, or in an accretionary wedge against the Sino-Korean craton; all of these possibilities remain viable. By far the greatest divergence of opinion centers on the amphibolite and migmatite units. Neither of these units preserves evidence of metamorphism at high pressures; so their relationships to the HP units are uncertain. Two recent tectonic models (Okay and Şengör, 1992; Liou et al., Chapter 15, this volume) underscore this difficulty by omitting the amphibolite unit from their tectonic reconstructions. The migmatite unit has been postulated as part of the Sino-Korean craton in the hanging wall of the subduction zone (Liou, et al., Chapter 15, this volume), as a pre-collisional arc formed on the margin of the Sino-Korean craton (Cong et al., 1994), and as a less deeply subducted portion of the Yangtze craton (Okay and Şengör, 1992). Again, all these hypotheses are viable, although the latter is difficult to envision; if temperatures were above 800°C at 20–60 km of depth in the Yangtze craton (conditions for migmatization), temperatures at 120–140 km of depth (conditions for diamond formation) would be unlikely to have been the same, even within a subduction zone. Note that the suture between the two cratons varies in these tectonic models from the northern boundary of the Foziling "Group" (Okay and Şengör, 1992) to the southern boundary of the migmatite unit (Liou et al., Chapter 15, this volume).

The postulated means by which the UHP rocks were exhumed fall into two familiar categories: thrusting and coeval erosion, and normal faulting. Both models assume that the UHP rocks were displaced upward in response to continued shortening between the Sino-Korean and Yangtze cratons. The thrust model is exemplified by the theory of Okay and Şengör (1992), who view the Dabie Shan as a wedge bounded below by a north-dipping basal décollement that breached the surface at the southern edge of the fold-thrust belt, and bounded above by the subduction thrust beneath the Sino-Korean hanging wall (subsequently back-folded into a steep southward dip). They suggest that the migmatite unit was a part of the down-going Yangtze plate that was thrust northward beneath the eclogite unit. Moreover, they postulate that the pervasive south-dipping structures within the Dabie Shan and the exposure of migmatite *north* of the eclogite were both caused by late Triassic large-scale doming during readjustment of the lithosphere following detachment of a dense orogenic root. In this model, exposure of the eclogites depends ultimately on erosion. The Cretaceous granites are envisioned as late-stage crustal melts produced by crustal thickening (Okay et al., 1993).

The "extrusion" model of Liou et al. (Chapter 15, this volume) shows the Dabie UHP rocks as a thick sheet bounded below by the same basal thrust used by Okay et al. (1993) and bounded above by a lithosphere-scale normal fault. They suggest that the migmatite unit was a part of the hanging wall of the Sino-Korean plate, reached its peak temperatures in Jurassic–Cretaceous time, and that the migmatite/eclogite contact changed from a north-dipping thrust during subduction to a normal fault during orogenic collapse. Note that the apparent south dip of this structure (Figure 16.2) is in conflict with their model. Like Okay et al. (1993), they called upon doming across the entire orogen to explain the pervasive south-dipping structures within the Dabie Shan, but they suggested Jurassic–Cretaceous doming coincident with the intrusion of late-stage crustal melts.

To summarize, the main differences between the models of Okay et al. (1993) and Liou et al. (Chapter 15, this volume) that can be tested are (1) the time of migmatization (early Triassic vs. Jurassic–Cretaceous), (2) the time of doming (late Triassic vs. Jurassic–Cretaceous), and (3) the sense of displacement along the migmatite/eclogite contact. Okay et al. (1993) propose that the eclogite unit was always moving south over the migmatite unit, but because of late Triassic doming, that contact was a north-dipping thrust fault in the early Triassic and a south-dipping normal fault in the late Triassic. Liou et al. (Chapter 15, this volume) propose that this contact was always north-dipping but was an early Triassic thrust fault and a late Triassic normal fault.

### *An Alpine model*

As a further illustration of the range of tectonic possibilities permitted by the currently sparse data, we propose another model based on an inferred evolution of the central and eastern Alps (Merle and Guillier, 1989; Pfiffner et al., 1990; Ratschbacher et al., 1991). The diamond- and coesite-bearing rocks in the Dabie Shan are separated by more than 1.0 GPa of metamorphic pressure, and they formed at about 130 km and 80 km, respectively. If the diamond-bearing eclogites are knockers within a lower-pressure coesite-bearing eclogite terrane and were brought upward during subduction by entrainment in less dense material undergoing return flow during subduction (Cloos, 1982) then the extreme depths from which they had to be exhumed can be reduced by about 50 km (Figure 16.8A). This prediction conceivably could be tested by observing whether the structures around the margins of diamond-bearing eclogite blocks indicate symmetric or asymmetric flow fields, and by determining whether the 1.0-GPa gap in pressure was real or whether peak depths in the 80–130 km range were reached. If no rocks are found with peak metamorphic pressures in the 3.2–3.8-GPa range, then the diamond-bearing rocks would appear to be knockers.

Rather than having required the stacking of multiple 35–50-km-thick sections of continental crust to achieve ultra-high pressures, the continental material that was subducted to 100–130 km may have been much thinner. Transitional crust, which can be about 10 km thick and several hundred kilometers wide around continents, can easily be subducted to mantle depths. It is only when continental crust thicker than about 20 km is forced to subduct that buoyancy of the lithosphere arrests underthrusting (Cloos, 1982). When positively buoyant lithosphere stalls subduction, the positively and negatively buoyant subducted material can separate, allowing the buoyant portions (i.e., continental crust) to rise (Sacks and Secor, 1990). The change from downward to upward vertical motion can occur by pure shear horizontal stretching and vertical thinning of the upper plate (Platt, 1986; Behrmann and Ratschbacher, 1989) (Figure 16.8B). It might even be accelerated by coincident deeper tectonic underplating (Platt, 1986), which also would have the desirable feature of depressing temperatures at depth (Hacker and Peacock, 1994). This phase of deformation can entirely precede the main collisional event. If vertical thinning on the order of 50% were to occur, rocks formed at 80 km of depth might be exhumed to about 40 km by tectonic processes alone. Our suggestion can be tested by looking for homogeneous coaxial deformation beginning at peak metamorphic pressures and continuing through early decompression, as Behrmann and Ratschbacher (1989) tested the eclogitic rocks in the Tauern Window of the eastern Alps.

The final stage of exhumation recognized in the central Alps (Merle and Guillier, 1989) was vertical extrustion, permitted by thermal weakening of the tectonically thickened part of the orogen. During the approximately 10–30 m.y. following any thrusting, thickened crust will be abnormally strong because of depressed temperatures; subsequent to that, thermal equilibrium will be reestablished at abnormally high temperatures because of the double thickness of radiogenic material (England and Thompson, 1984; Glazner and Bartley, 1985). Heating will lead to weakening of the previously strong parts of the collision zone, raising the possibility that deformation will migrate into the newly weakened area. Such a scenario has been proposed for the Swiss Alps, where eo-Alpine HP metamorphism at 100 Ma or earlier was followed by a lull of about 50 m.y., and then by renewed deformation and plutonism (Merle and Guillier, 1989). That late deformation was triggered by contraction as the Adriatic sub-plate acted as a rigid indenter against the European plate and produced large-scale recumbent nappes and overturning of earlier structures developed within oceanic and continental fragments trapped between the cratons (Merle and Guillier, 1989; Pfiffner et al., 1990). In the Dabie Shan, there may have been a similar orogenic lull between about 180 Ma, when UHP rocks cooled, and 135 Ma, when widespread plutonism and late deformation began.

To apply the Alpine model to the Dabie Shan, we suggest that the Sino-Korean craton acted as a rigid indenter into the stacked crust at the leading edge of the Yangtze craton and produced large-scale recumbent nappes and overturning of earlier structures developed within an orogenic wedge between the cratons (Figure 16.8C). The indentation would have produced overturning of originally north-dipping structures in the underplated Yangtze crust and a new foliation due to the northward flow of extruded Yangtze crust onto the Sino-Korean craton; deformation would have been accompanied by Barrovian-type metamor-

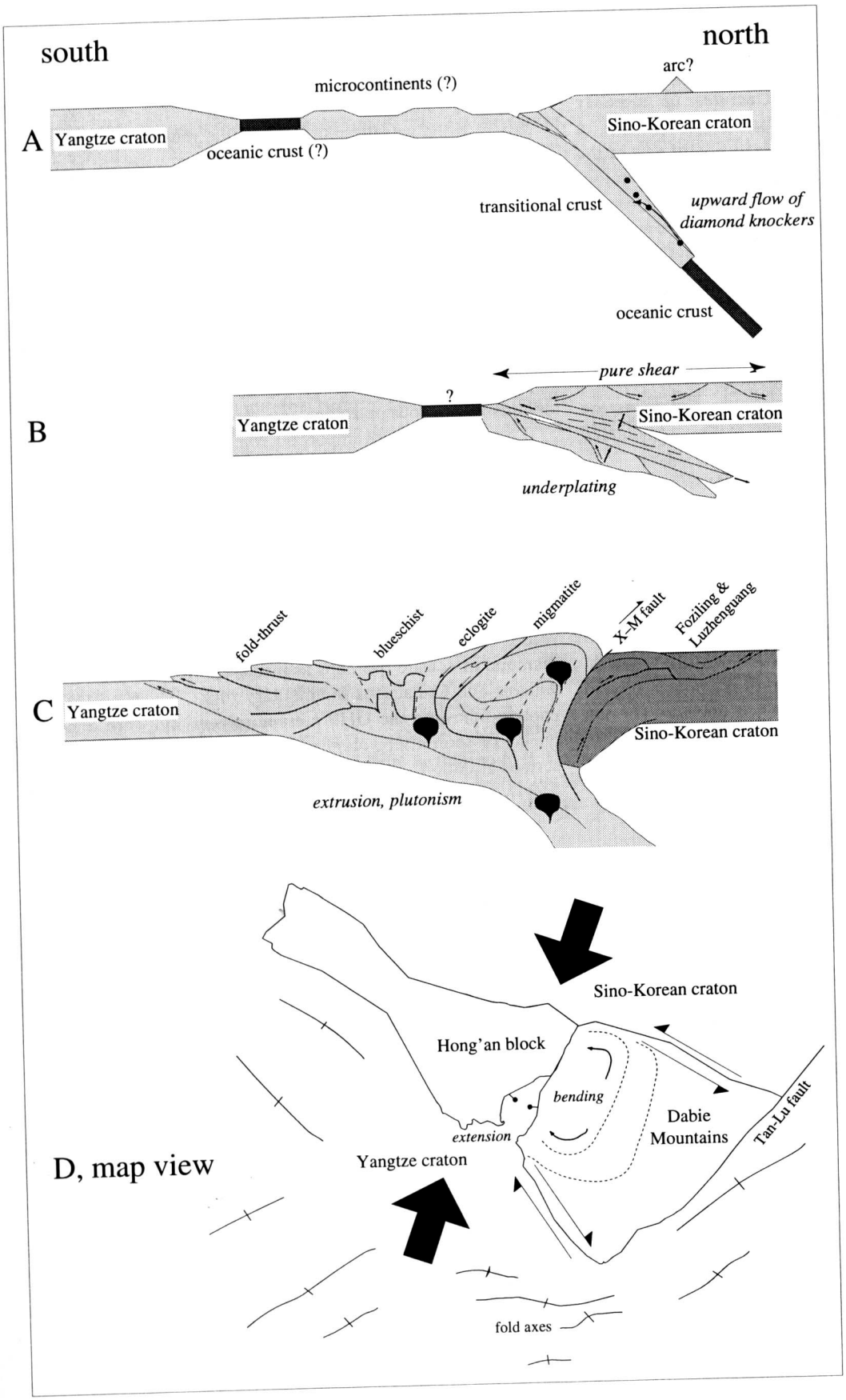


**Figure 16.8. Alpine model for the Dabie Shan. (A) Possible exhumation of diamond-bearing rocks to about 90 km of depth. (B) Possible exhumation by vertical shortening, horizontal extension, and underplating. (C) Possible indentation by Sino-Korean craton into thermally equilibrated and weakened orogen core causes vertical extrusion and overturning of earlier structures, coincident with magmatism. (D) Possible horizontal, eastward extrusion of the Hong'an and Dabie blocks.**

phism. The root zone of upwelling could be represented by the dome within the migmatite unit, and the south-dipping foliations within the eclogite and amphibolite units (but, importantly, not in the blueschist and fold-thrust belt) could represent either overturned, originally north-dipping structures or a newly developed fabric. The vertical-extrusion model predicts a bivergent orogenic belt, with northward extrusion of part of the orogenic wedge tens of kilometers onto the Sino-Korean craton, and especially the Yangtze craton, and about 30 km of vertical exhumation in the core of the orogen similar to an interpretation of the Alps (Pfiffner et al., 1990). Both cratons should also contain craton-directed fold-thrust belts formed at that time. This model predicts the development of specific structures that postdate peak metamorphic pressures. Additionally, loss of the dense lithospheric root and asthenospheric upwelling are predicted to have caused intrusion of the widespread granitoids and partial melting in the migmatite unit; plutons and dikes are inferred to be derived from asthenospheric melts contaminated by melting of crustal rocks.

The final exhumation of rocks in this postulated history may have been by lateral extrusion (Tapponnier, Peltzer, and Armijo, 1986), akin to that postulated for the eastern Alps (Ratschbacher et al., 1991) (Figure 16.8D). Because of weak boundaries with the Pacific place farther east, convergence between the Sino-Korean and Yangtze cratons could have resulted in the Dabie Shan being extruded eastward. If so, the northern and southern boundaries of the Dabie Shan should be left- and right-lateral strike-slip faults, respectively. Other features potentially related to eastward extrusion of the Dabie Shan include (1) the counterclockwise and clockwise bending of structural trend lines in the northern and southern Dabie Shan as a result of doming of buoyant crusts within the tensional quadrant of the eastward-escaping block; (2) the westward-tapering wedge shape of the Dabie and Hong'an blocks; (3) the extensional basin separating the Dabie and Hong'an blocks; (4) the change in fold axes in the Yangtze-craton fold-thrust belt from WNW west of the Tan Lu fault to NE east of the Tan Lu fault (fig. 2 of Yin and Nie, 1993), and (5) the southward displacement of the Qinling–Dabie belt relative to the Sulu area.

Of course, the model we have described is speculative and reaches far beyond the available data – our intention is only to indicate the range of possibilities and illustrate the variety of hypothetical situations that must be tested. Testing these drastically different models for the Qinling–Dabie belt (Hacker et al., 1995) will ultimately tell us much about the evolution of collisional orogens in general.

### Questions

In summary, tectonic models are not yet well constrained; there is an urgent need for input from observations and interpretations of the rocks themselves. We close with a few salient questions that we hope will focus attention on key unresolved issues.

What is the timing relationship between the partial melting in the migmatite unit and the UHP metamorphism? Were the migmatitic rocks subjected to ultra-high pressures? Answers to these questions will require mapping to differentiate the various plutonic and meta-plutonic rocks in the migmatite unit, an understanding of their igneous and metamorphic petrology, and U-Pb isotope studies.

Where is the volcano-plutonic arc that must have been active during subduction prior to collision? What were the compositional history and volumetric-eruption history of this arc? Radiometric investigation of potential volcano-plutonic rocks is urgently required.

What are the ages and compositions of the Jurassic and Cretaceous plutons and volcanic rocks? Are they related to the collisional orogeny, or are they responsible for the late Barrovian overprint on the UHP rocks? If the collision and the younger plutons are related, what was responsible for the apparent interregnum of 60–80 m.y.? These issues involve dominantly igneous petrology and geochronology.

If erosion played an important role in exhuming the rocks in the Dabie Shan, where are the sediments that would have come from the 100-km-thick section that lay above the UHP rocks? What aspects of the exhumation history do they record? The Songpan–Ganzi basin southwest of the orogen has been suggested as the likely candidate (Yin and Nie, 1993; Zhou and Graham, 1993; Zhou and Graham, Chapter 14, this volume), but few details are known. The Songpan–Ganzi basin may contain a record of unroofing of the UHP rocks in the form of detrital diamond or coesite (perhaps as inclusions in other phases). The Jurassic and Cretaceous sedimentary rocks, which postdate the cooling following the UHP metamorphism and were deposited during or soon after voluminous volcano-plutonism, also merit serious attention.

Why is there such non-systematic discordance and apparent complexity among the various isotope systems used to date various stages of the UHP metamorphism? Because much of the important activity in the orogen took place at elevated temperatures, extensive use of the U-Pb decay scheme, with its high closure temperatures, is required. Mapping to determine whether or not post-metamorphic structures separate rocks with notably different radiometric ages will also be critical.

What structures testify to the exhumation process, and at what rates and when were they active? The obvious high-angle faults that segment the orogen into narrow E–W-trending belts serve to distract attention from the large-scale low-angle faults that must have been active during exhumation. It is these "cryptic" faults that must be understood. At present, our field observations of the Xiautian–Mozitan fault and the migmatite/eclogite fault would seem to preclude either from having had a major role in exhuming the UHP rocks from depths in excess of 100 km. Whatever structures were responsible have remained unexposed or undiscovered or have been overprinted by younger deformation.

Preservation of UHP minerals requires that thermal re-equilibration be suppressed, either (1) by rapid exhumation to shallow-crustal levels and lower temperatures or, if the exhumation rate is slow, (2) by concomitant deeper-level subduction (Ernst, 1977; Hacker and Peacock, 1994). At present, both

options remain viable. Thus far, our radiometric age data do not precisely define a narrow interval of rapid cooling that might plausibly be linked with rapid decompression.

Why, if the Dabie Shan comprise a subducted portion of the Yangtze craton, as is commonly assumed, do the structures within much of the Dabie Shan verge to the north? The hot-eclogite, cold-eclogite, and amphibolite units, and possibly the blueschist unit, all feature south-dipping foliation, and each more southerly and lower-pressure unit apparently lies structurally above the next higher-pressure unit to the north along south-dipping contacts. This is one of many large-scale questions that can be addressed a few years from now as answers from these other multidisciplinary studies become available.

Is the current distribution of HP and UHP rocks the result of exhumation subduction? In other words, is it possible that subduction of continental material occurred along a great length of the orogen from the Qinling Shan to the Sulu area, but subsequent exhumation of those rocks was greatest in the Sulu and Dabie Shan and progressively weaker in areas farther west? Or did one of the cratons have a promontory that was subducted to profound depths and then exhumed in almost its entirety (Yin and Nie, 1993)?

Answers to all these questions will be required before the central issue – understanding the creation, preservation, and exhumation of UHP rocks in collisional orogens – can be satisfactorily resolved.

### Acknowledgments

Our work in China has been enthusiastically facilitated by J. G. Liou, R. G. Coleman, and S. A. Graham. Field work in 1992 was supported by Academia Sinica, most notably Wang Qingchen, Liu Xiaohan, and Cong Bolin. Helpful reviews were provided by G. A. Davis, H. W. Day, Jun Liu, and Xiaoming Zhai. Funding for this research came from NSF grant EAR-9204563 and the Stanford–China Earth Sciences Industrial Affiliates Program.

### References

Ames, L. 1993. Correlation of ultrahigh-pressure blocks based on timing of metamorphism as a result of continental collision in the Dabie suture zone, central China. *Geol. Soc. Am. Abstr. Prog.* 25:117.

Ames, L., Tilton, G. R., and Zhou, G. 1993. Timing of collision of the Sino-Korean and Yangtse cratons: U-Pb zircon dating of coesite-bearing eclogites. *Geology* 21:339–42.

Ames, L., Zhou, G., and Xiong, B. in press. Geochronology and geochemistry of ultrahigh-pressure metamorphism with implications for collision of the Sino-Korean and Yangtze cratons, central China. *Tectonics*

Behrmann, J. H., and Ratschbacher, L. 1989. Archimedes revisited: a structural test of eclogite emplacement models in the Austrian Alps. *Terra Nova* 1:242–52.

Buck, W. R., 1988. Flexural rotation of normal faults. *Tectonics* 7:959–73.

Chen, W., Harrison, T. M., Heizler, M. T., Liu, R., Ma, B., and Li, J. 1992. The cooling history of melange zone in north Jiangsu–south Shandong region: evidence from multiple diffusion domean $^{40}$AR-$^{39}$AR thermal geochronology. *Acta Petrol. Sinica* 8:1–17.

Chopin C. 1984. Coesite and pure pyrope in high-grade blueschists of the western Alps: a first record and some consequences. *Contrib. Mineral. Petrol.* 86:107–18.

Cloos, M. 1982. Flow melanges: numerical modeling and geologic constraints on their origin in the Franciscan subduction complex. *Geol. Soc. Am. Bull.* 93:330–45.

Cong. B. L., Wang, Q., Zhai, M., Zhang, R., and Ye, K. 1994. UHP metamorphic rocks on the Dabie–Su-Lu region, China: their formation and exhumation. *Island Arc* 3:135–50.

Dong, S. 1993. Metamorphic and tectonic domains of China. *Metamorphic Geol.* 11:465–81.

Dong, S., Shen, Q., Sun, D., and Lu, L. 1986. Metamorphic Map of China with an Explanatory Text, scale 1:4,000,000. Beijing: Geological Publishing House.

Dong, S. W., Sun, X. R., Zhang, Y., Huang, D. Z., Wang, G., Dai, S. K., and Yu, B. C. 1993. The basic structure of the Dabie collisional orogen. *Chinese Science Bulletin* 38:1884–8.

Du, D. 1986. *Research on the Devonian System of the Qin-Ba Region within the Territory of Shaanxi.* Xi'an: Jiaotang University Publishing House.

Eide, E. A. 1993. Petrology, geochronology, and structure of high-pressure metamorphic rocks in Hubei province, east-central China, and their relationship to continental collision. Ph.D. dissertation, Stanford University.

Eide, E. A., McWilliams, M. O., and Liou, J. G. 1994. $^{40}$Ar/$^{39}$Ar geochronology and exhumation of high-pressure to ultrahigh-pressure metamorphic rocks in east-central China. *Geology (Boulder)* 22:601–4.

Enami, M., and Zang, Q. 1990. Quartz pseudomorph after coesite in eclogites from Shandong province, east China. *Mineralogist* 75:381–6.

Enami, M., Zang, Q., and Yin, Y. 1993. High pressure eclogites in northern Jiagsu–southern Shandong province, east China. *J. Metamorphic Geol.* 11: 589–603.

England, P. C., and Thompson, A. B. 1984. Pressure–temperature–time paths of regional metamorphism. I: Heat transfer during the evolution of regions of thickened continental crust. *J. Petrol.* 25:894–928.

Enkin, R. J., Yang, Z., Chen, Y., and Courtillot, V. 1992. Paleomagnetic constraints on the geodynamic history of the major blocks of China from the Permian to the present. *J. Geophys. Res.* 97:13,953–89.

Ernst, W. G. 1977. Tectonics and prograde versus retrograde *P–T* trajectories of high-pressure metamorphic belts. *Rendiconti della Societa Italiana di Mineralogie a Petrologia* 33:191–220.

Ernst, W. G., Zhou, G. Liou, J. G., Eide, E., and Wang, X. 1991. High-pressure and superhigh-pressure metamorphic terranes in the Qinling–Dabie mountain belt, central China; early to mid-Phanerozoic accretion of the western Paleo-Pacific Rim. *Pacific Science Assoc. Inform. Bull.* 43:6–15.

Gao, S., Zhang, B. R., Luo, T. C., Li, Z. J., Xie, Q. L., Gu, X. M., Zhang, H. F., Ouyang, J. P., Wang, D. P., and Gao, C. L. 1992. Chemical composition of the continental crust in the Qinling orogenic belt and its adjacent North China and Yangtze cratons. *Geochim. Cosmochim. Acta* 56:3933–50.

Glazner, A. F., and Bartley, J. M. 1985. Evolution of lithospheric strength after thrusting. *Geology* 13:42–5.

Hacker, B. R. 1991. The role of deformation in the formation of metamorphic field gradients: ridge subduction beneath the Oman ophiolite. *Tectonics* 10:455–73.

Hacker, B. R., and Peacock, S. M. 1994. Creation, preservation, and exhumation of coesite-bearing, ultrahigh-pressure metamorphic rocks. In *Ultrahigh Pressure Metamorphism,* ed. R. G. Coleman and X. Wang, pp. 157–81. Cambridge University Press.

Hacker, B. R., Ratschbacher, L., Webb, L., Dong, S. W. 1995. What brought them up? Exhumation of the Dabie Shan ultra-high-pressure rocks. *Geology* 23:743–6.

Hacker, B. R., and Wang, Q. C. in press. Thermal history of ultrahigh-pressure rocks, Dabie Mountains, China. *Tectonics.* 14:994–1006.

Hao, Y. 1990. Accretion and dispersion of terranes in Hubei, China. In *Terrane Analysis of China and the Pacific Rim,* ed. T. J. Wiley, D. G. Howell, and F. L. Wong, pp. 275–9. Houston: Circum-Pacific Council for Energy and Mineral Resources.

Hsü, K. J., Li, J., Chen, H., Wang, Q., Sun, S., and Şengör, A. M. C. 1990. Tectonics of south China: key to understanding West Pacific geology. *Tectonophysics* 183:9–39.

Hsü, K. J., Wang, Q., Li, J., Zhou, D., and Sun, S. 1987. Tectonic evolution of the Qinling Mountains, China. *Eclogae Geol. Helv.* 809:735–52.

Hu, N., Yang, J., An, S., and Hu, J. 1993. Metamorphism and tectonic evolution of the Shangdan fault zone, Shaanxi, China. *J. Metamorphic Geol.* 11:537–48.

Huang, W. 1993. Multiphase deformation and displacement within a basement complex on a continental margin: the Wudang Complex in the Qinling orogen, China. *Tectonophysics* 224:305–26.

Huang, W., and Wu., Z. W. 1992. Evolution of the Qinling orogenic belt. *Tectonics* 11:371–80.

Jamtveit, B., Bucher-Nurminen, K., and Austrheim, H. 1990. Fluid controlled eclogitization of granulites in deep crustal shear zones, Bergen arcs, western Norway. *Contrib. Mineral. Petrol.* 104:184–93.

Jin, F. 1989. Carboniferous paleogeogrpahy and paleoenvironment between the North and South China blocks in eastern China. *Southeast Asian Earth Sci.* 3:219–22.

Kröner, A., Compston, W., Zhang, G. W., Guo, A. L., and Todt, W. 1988. Age and tectonic setting of late Archean greenstone-gneiss terrane in Henan province, China, as revealed by single-grain zircon dating. *Geology* 16:211–15.

Kröner, A., Zhang, G. W., and Sun, Y. 1993. Granulites in the Tongbai area, Qinling belt, China: geochemistry, petrology, single zircon geochronology, and implications for the tectonic evolution of eastern Asia. *Tectonics* 12:245–55.

Kullerud, L., Tørudbakken, R. O., and Ilebekk, S. 1986. A compilation of radiometric age determinations from the Western Gneiss Region, south Norway. *Norges Geologiske Undersøkelse Bulletin* 406:17–42.

Lerch, M. F., Xue, F., Kröner, A., Zhang, G. W., and Todt, W. 1995. A Middle Silurian–early Devonian magmatic arc in the Qinling Mountains of central China. *J. Geol.*

Li, C., Ma, J., Chen, R., and Zhao, J. 1990. New recognition of the stratigraphic sequence and age of the Erlanping Group in Henan Province. *Regional Geol. China* 1990:181–5.

Li, S., Liu, D., Chen, Y., Wang, S., Qiu, J., Hu, S., and Sang, H. 1993a. Time of the blueschist belt formation in central China. *Scientia Geologica Sinica* 28:21–7.

Li, S., and Wang, T. 1991. *Geochemistry of Granitoids in the Tongbaishan-Dabieshan, Central China.* Wuhan: China University of Geosciences Press.

Li, S., Wang, S., Chen, Y., Liu, D., Qiu, J., Zhou, H., and Zhang, Z. 1994. Excess argon in phengite from eclogite: evidence from the dating of eclogite minerals by the Sm-Nd, Rb-Sr and $^{40}Ar/^{39}Ar$ methods. *Chem. Geol.* 112:343.

Li, S., Xiao, Y., Liou, D., Chen, Y., Ge, N., Zhang, Z., Sun, S.-S., Cong, B., Zhang, R., Hart, S. R., and Wang, S. 1993b. Collision of the North China and Yangtze blocks and formation of coesite-bearing eclogites: timing and processes. *Chem. Geol.* 109:89–111.

Li, S. G., Ge, N., Liu, D. L., Zhang, Z., Yie, X. J., Zhen, S. G., and Peng, C. Q. 1989a. Sm-Nd age of C-group eclogites in the northern Dabie Mountains and its tectonic significance (in Chinese). *Bulletin of Science* 7:522–5.

Li, S. G., Hart, S. R. Zheng, S. G., Liou, D. L., and Guo, A. 1989b. Sm-Nd isotopic evidence for the timing of the collision between the north and south China cratons – the Sm-Nd isotopic evidence. *Science in China* 32:1391–400.

Li, S. G., Hart, S. R., Zheng, S. G., Liu, D. L., Zhang, G. W., and Guo, A. L. 1989c. Timing of collision between the north and south China blocks – the Sm-Nd isotopic age evidence. *Science in China* 32:1393–1400.

Lin, J. L., and Fuller, M. 1990. Paleomagnetic constraints on relative motions of the Asian blocks and terranes. In *Terrane Analysis of China and the Pacific Rim,* ed. T. J. Wiley, D. G. Howell, and F. L. Wong, pp. 195–210. Houston: Circum-Pacific Council for Energy and Mineral Resources.

Liu, Q., and Shan G. 1992. Geophysical properties of the lower crustal granulites from the Qinling orogenic belt, China. *Tectonophysics* 204:401–8.

Liu, X., and Hao, J. 1989a. The framework and tectonic evolution of east Qinling belt (Tongbai–Dabie mountains) in east China. *Advances in Geosciences, Contributions to 28th International Geological Congress* 1:34–47.

Liu, X., and Hao, J. 1989b. Structure and tectonic evolution of the Tongbai–Dabie range in the East Qinling collisional belt, China. *Tectonics* 8:637–745.

Liu, Y., Nutman, A. P., Compston, W., Wu, J. S., and Shen, Q. H. 1992. Remnants of ≥ 3800 Ma crust in the Chinese part of the Sino-Korean craton. *Geology* 20:339–42.

Ma, B., and Zhang, Z. 1988. The features of the paired metamorphic belts and evolution of paleotectonics in the east part of Dabie Mountains (in Chinese). *Seismology and Geology* 10:19–28.

Ma, W. 1989. Tectonics of the Tongbai–Dabie fold belt. *J. Southeast Asian Earth Sci.* 3:77–85.

Ma, W. 1991. The Carboniferous at the northern foot of the Dabie Mountains and its tectonic implications. *Acta Geol. Sinica* 4:237–49.

Ma, X. Y. 1986. *Geodynamic Map of China, scale 1 : 4,000,000.* Beijing: Geological Publishing House.

Maruyama, S., Liou, J. G., Zhang, R. 1994. Tectonic evolution of the ultrahigh-pressure (UHP) and high-pressure (HP) metamorphic belts from central China. *Island Arc* 3:112–21.

Mattauer, M., Matte, P., Malavieille, J., Tapponnier, P., Maluski, H., Xu, Z. Q., Lu, Y. L., and Tang, Y. Q. 1985. Tectonics of the Qinling belt: build-up and evolution of eastern Asia. *Nature* 317:496–500.

Mattauer, M., Matte, P., Maluski, H., Xu, Z., Zhang, Q. W., and Wang, Y. M. 1991. La limite Chine du Nord-Chine du Sud au Paléozoïque et au Trias. Nouvelles données structurales et radiométriques dans le massif de Dabie-Shan (chaîne des Qinling) (Paleozoic and Triassic plate boundary between North and South China: new structural

and radiometric data on the Dabie-Shan, eastern China). *C. R. Acad. Sci., Sér. 2* 312:1227–33.

Merle, O., and Guillier, B. 1989. The building of the central Swiss Alps: an experimental approach. *Tectonophysics* 165:41–56.

Monié, P., and Chopin, C. 1991. $^{40}Ar/^{39}Ar$ dating in coesite-bearing and associated units of the Dora Maira massif, western Alps. *Eur. J. Mineral.* 3:239–62.

Morgan, P. 1984. The thermal structure and thermal evolution of the continental lithosphere. *Phys. Chem. Earth* 15:107–93.

Okay, A. I. 1993a. Petrology of a diamond and coesite-bearing metamorphic terrain: Dabie Shan, China. *Eur. J. Mineral.* 5:569–75.

Okay, A. I. 1993b. Sapphirine and Ti-clinohumite in ultra-high-pressure garnet-pyroxenite and eclogite from Dabie Shan, China. *Contrib. Mineral. Petrol.* 110:1–13.

Okay, A. I., and Şengör, A. M. C. 1992. Evidence for intracontinental thrust-related exhumation of the ultra-high-pressure rocks in China. *Geology* 20:411–14.

Okay, A. I., Şengör, A. M. C., and Satir, M. 1993. Tectonics of an ultrahigh-pressure metamorphic terrane: the Dabie Shan/Tongbai Shan orogen, China. *Tectonics* 12:1320–34.

Okay, A. I., Xu, S. T., Şengör, A. M. C. 1989. Coesite from the Dabie Shan eclogites, central China. *Eur. J. Mineral.* 1:595–8.

Pearson, N. J., O'Reilly, S. Y., and Griffin, W. L. 1991. The granulite to eclogite transition beneath the eastern margin of the Australian craton. *Eur. J. Mineral.* 3:293–322.

Peltzer, G., Tapponnier, P., Zhang, Z., and Xu, Z. Q. 1985. Neogene and Quaternary faulting in and along the Qinling Shan. *Nature* 317:500–5.

Pfiffner, O. A., Frei, W., Valasek, P., Stäuble, M., Levato, L., DuBois, L., Schmid, S. M., and Smithson, S. B. 1990. Crustal shortening in the Alpine orogen: results from deep seismic reflection profiling in the eastern Swiss Alpes, line NFP 20-east. *Tectonics* 9:1327–55.

Platt, J. P. 1986. Dynamics of orogenic wedges and the uplift of high-pressure metamorphic rocks. *Geol. Soc. Am. Bull.* 97:1037–53.

Ratschbacher, L., Frisch, W., Linzer, H. -G., and Merle, O. 1991. Lateral extrusion in the eastern Alps. Part 2: Structural analysis. *Tectonics* 10:257–71.

Reischmann, T., Altenberger, U., Kröner, A., Zhang, G., Sun, Y., and Yu, Z. 1990. Mechanism and time of deformation and metamorphism of mylonitic orthogneisses from the Shagou shear zone, Qinling belt, China. *Tectonophysics* 185:91–109.

R.G.S. Anhui. *Regional Geology of Anhui Province (in Chinese)*. Beijing: Geological Publishing House.

R.G.S. Henan. 1989. *Regional Geology of Henan Province* (in Chinese). Beijing: Geological Publishing House.

R.G.S. Hubei. 1990. *Regional Geology of Hubei Province* (in Chinese). Beijing: Geological Publishing House.

R.G.S. Shaanxi. 1989. *Regional Geology of Shaanxi Province* (in Chinese). Beijing: Geological Publishing House.

Sacks, P. E., and Secor, D. T. 1990. Delamination in collisional orogens. *Geology* 18:999–1002.

Sang, B., Chen, Y., and Shao, G. 1987. The Rb-Sr ages of metamorphic series of the Susong Group at the southeastern foot of the Dabie Mountains, Anhui province, and their tectonic significance. *Regional Geol. China* 4:364–70.

Smith, D. C. 1984. Coesite in clinopyroxene in the Caledonides and its implications for geodynamics. *Nature* 310:641–4.

Tapponnier, P., Peltzer, G., and Armijo, R. 1986. On the mechanics of the collision between India and Asia. In *Collision Tectonics*, ed. M. P. Coward and A. C. Ries, pp. 115–57. London: Geological Society.

Tilton, G. R., Schreyer, and Schertl, H. -P. 1991. Pb-Sr-Nd isotopic behavior of deeply subducted crustal rocks from the Dora Maira massif, western Alps, Italy. II: What is the age of the ultrahigh pressure metamorphism. *Contrib. Mineral. Petrol.* 108:22–33.

Wang, N. 1989. Micropaleontological study of lower Paleozoic siliceous sequences of the Yangtze platform and eastern Qinling Range. *J. Southeast Asian Earth Sci.* 3:141–61.

Wang, X. 1991. Petrology of coesite-bearing eclogites and ultramafic rocks from ultrahigh-pressure metamorphic terrane of the Dabie Mountains and implications to regional tectonics in central China, Ph.D. dissertation, Stanford University.

Wang, X., Jing., Y., Liou, J. G., Pan, G., Liang, W., Xia, M., and Maruyama, S. 1990. Field occurrences and petrology of eclogites from the Dabie Mountains, Anhui, central China. *Lithos* 25:119–31.

Wang, X., and Liou, J. G. 1991. Regional ultrahigh-pressure coesite-bearing eclogitic terrane in central China: evidence from country rocks, gneiss, marble, and metapelite. *Geology* 19:933–6.

Wang, X., and Liou, J. G. 1993. Ultrahigh-pressure metamorphism of carbonate rocks in the Dabie Mountains, central China. *J. Metamorphic Geol.* 11:575–88.

Wang, X., Liou, J. G. and Mao, H. K. 1989. Coesite-bearing eclogite from the Dabie Mountains in central China. *Geology* 17:1085–8.

Wang X., Liou, J. G., and Maruyama, S. 1992. Coesite-bearing eclogite from the Dabie Mountains, central China: petrology and *P–T* path. *J. Geol.* 100:231–50.

Wdowinski, S., and Axen, G. J. 1992. Isostatic rebound due to tectonic denudation: a viscous flow model of a layered lithosphere. *Tectonics* 11:303–15.

Wever, T., and Sadowiak P. 1989. A relationship between crustal thickness and mean crustal velocity. *Tectonophysics* 170:159–63.

Xu, S., Jiang, L., Liu, Y., and Zhang, Y. 1992a. Tectonic framework and evolution of the Dabie Mountains in Anhui, eastern China. *Acta Geol. Sinica* 66:1–14.

Xu, S., Okay, A. I., Ji, S., Şengör A. M. C., Su, W., Liu, Y., and Jiang, L. 1992b. Diamond from the Dabie Shan metamorphic rocks and its implication for the tectonic setting. *Science* 256:80–2.

Xu, S., Zhou, H. Dong, S., Chen, G., and Zhang, W. 1986. Deformation and evolution of the predominant structural elements in Anhui Province, China (in Chinese). *Scientia Geologica Sinica* 2:311–22.

Yang, Z., Cheng, Y., and Wang, H. 1986. *The Geology of China*. Oxford: Clarendon Press.

Yin, A., and Nie, S. 1993. An indentation model for the North and South China collision and the development of the Tanlu and Honam fault systems, eastern Asia. *Tectonics* 12:801–13.

You, Z., Han, Y., Suo, S., Chen, N., and Zhong, Z. 1993. Metamorphic history and tectonic evolution of the Qinling Complex, eastern Qinling Mountains, China. *J. Metamorphic Geol.* 11:549–60.

Zhai, X., Day, H. W., and Hacker, B. R. 1995. Multiple collisions in the Qinling orogenic belt: $^{40}Ar/^{39}Ar$ evidence in the north Tongbai Mts., Central China. *Geol. Soc. Am. Abstr. Progr.* 27:A456.

Zhang, G., Yu, Z., Sun, Y., Cheng, S., Li, T., Xue, F., and Zhang, C. 1989. The major suture zone of the Qinling orogenic belt. *J. Southeast Asian Earth Sci.* 3:63–76.

Zhang, G. W., Bai, Y. B., Sun, Y., Guo, A. L., Zhou, D. W., and Li, T. H. 1985. Composition and evolution of the Archaean crust in central Henan, China. *Precambrian Res.* 27:7–35.

Zhang, R. Y., and Liou, J. G. 1994. Coesite-bearing eclogite in Henan province, central China: detailed petrography, glaucophane stability and *PT*-path. *Eur. J. Mineral.* 6:217–33.

Zhang, R. Y., Liou, J. G., and Cong, B. 1994. Petrogenesis of garnet-bearing ultramafic rocks and associated eclogites in the Su-Lu ultrahigh-*P* metamorphic terrane, eastern China. *J. Metamorphic Geol.* 12:169–86.

Zhang, Z. M., Liou, J. G., and Coleman, R. G. 1984. An outline of the plate tectonics of China. *Geol. Soc. Am. Bull.* 95:295–312.

Zhao, X., and Coe, R. S. 1987. Palaeomagnetic constraints on the collision and rotation of North and South China. *Nature* 327:141–4.

Zhong, Z., You, Z., and Suo, S. 1990. Petrological study on the ductile shear zones in the core of the eastern Qinling orogenic belt in western Henan. *Acta Geol. Sinica* 3:379–91.

Zhou, D., and Graham, S. A. 1993. Songpan–Ganzi Triassic flysch complex as a remnant ocean basin along diachronous Qinling collisional orogen, central China. *Geol. Soc. Am. Abstr. Prog.* 25:A118.

Zhou, G., Liu, J., Eide, E. A., Liou J. G., and Ernst, W. G. 1993. High-pressure/low-temperature metamorphism in northern Hubei Province, central China. *J. Metamorphic Geol.* 11:561–74.